

Nucleophilic Aromatic Substitution in Hydrodefluorination Exemplified by Hydrido-iridium(III) Complexes with Fluorinated Phenylsulfonyl-1,2-diphenylethylenediamine Ligands

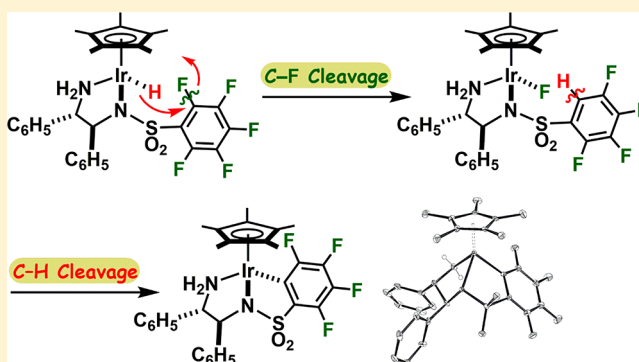
Asuka Matsunami,[†] Yoshihito Kayaki,^{*,†,‡} Shigeki Kuwata,^{†,‡,§} and Takao Ikariya^{†,#}

[†]Department of Chemical Science and Engineering, School of Materials and Chemical Technology, Tokyo Institute of Technology, O-okayama 2-12-1-E4-1, Meguro-ku, Tokyo 152-8552, Japan

[‡]PRESTO, Japan Science and Technology Agency (JST), 4-1-8 Honcho, Kawaguchi, Saitama 332-0012, Japan

Supporting Information

ABSTRACT: In connection with the mechanism of the catalytic reduction of fluoroarenes, the intramolecular defluorinative transformation of a family of iridium hydrides utilized as a hydrogen transfer catalyst is studied. Hydrido-iridium(III) complexes bearing fluorinated phenylsulfonyl-1,2-diphenylethylenediamine ligands are spontaneously converted into iridacycles via selective C–F bond cleavage at the *ortho* position. NMR spectroscopic studies and synthesis of intermediate model compounds verify the stepwise pathway involving intramolecular substitution of the *ortho*-fluorine atom by the hydrido ligand, i.e., hydrodefluorination (HDF), and the following fluoride-assisted cyclometalation at the transiently formed C–H bond. A hydrido-iridium complex with a 2,3,4,5,6-pentafluorophenylsulfonyl (Fs) substituent is more susceptible to HDF than its analog with a 2,3,4,5-tetrafluorophenylsulfonyl (Fs^H) group. The Fs^H-derivative clearly shows that C–F bond cleavage occurs in preference to C–H activation. These experimental results firmly support the nucleophilic aromatic substitution (S_NAr) mechanism in HDF by hydrido-iridium species.



INTRODUCTION

The development of convenient synthetic approaches to fluorinated organic compounds is essential because these chemicals are in great demand within the polymer, pharmaceutical, and agrochemical industries.¹ Perfluorinated aromatic chemicals are readily available on an industrial scale using fluorine gas or hydrogen fluoride, whereas the concise synthesis of partially fluorinated aromatic compounds is currently under development. Aside from monofluorination² accomplished using mild electrophilic reagents, i.e., NFSI or Selectfluor, and a versatile source of silver fluorides, the site-selective transformation of C–F bonds on perfluoroarenes is projected as one of the most profitable practical applications.

Transition-metal-mediated hydrodefluorination (HDF)³ of perfluoroarenes has received particular attention as a promising method to access partially fluorinated compounds. Many catalytic HDF systems have emerged primarily using hydrogen gas or fluorophilic reducing agents of hydrosilanes,⁴ boron hydrides,⁵ and aluminum hydrides.⁶ In regard to the limited applications of transfer hydrogenation to defluorinative reduction processes using alcohols^{7,8} or formate salts⁹ as mild reducing agents, we recently developed HDF of perfluorinated aromatic compounds catalyzed by bifunctional iridium complexes derived from primary benzylic amines.¹⁰ The

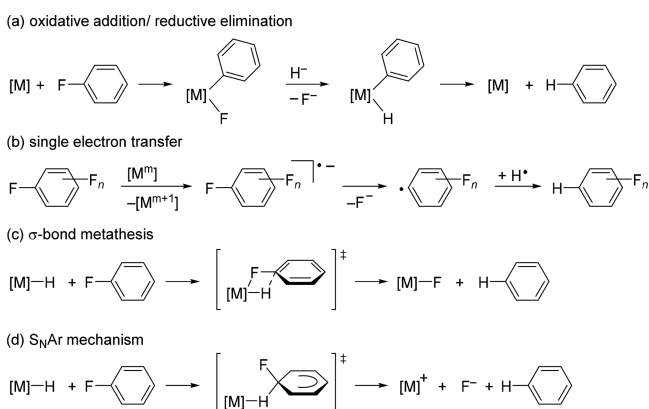
catalytically active hydrido-iridium complex possessing a σ -donating aryl-metal bond and a protic amine ligand engaged in an efficient catalytic HDF at ambient temperature, leading to outstanding activity and regioselectivity.

For C–F bond cleavage^{3b,11} of fluoroarenes in such reductive transformations, four types of mechanisms are typically proposed (Scheme 1): (a) oxidative addition to the transition metals followed by reductive elimination,^{4f,5a,12} (b) a single electron transfer radical mechanism,^{3a,11d,13} (c) σ -bond metathesis,^{14,15} and (d) nucleophilic substitution mediated by hydrides (S_NAr-like mechanism).^{3b} In general, explicitly determining the operative pathway in a catalytic HDF reaction is difficult.

Although numerous examples have demonstrated the oxidative addition of aromatic C–F bonds to a variety of low-valent metal species, the difference in the defluorinative processes between σ -bond metathesis and nucleophilic substitution is subtle, causing difficulty discerning these two mechanisms.¹⁶ Limited reports have discussed a nucleophilic substitution mechanism by hydrido ligands (Scheme 1d),^{3b} which can be linked to the rarity of well-defined metal hydride

Received: April 18, 2018

Scheme 1. Possible Pathways for the HDF of Fluoroarenes Using Transition-Metal Catalysts

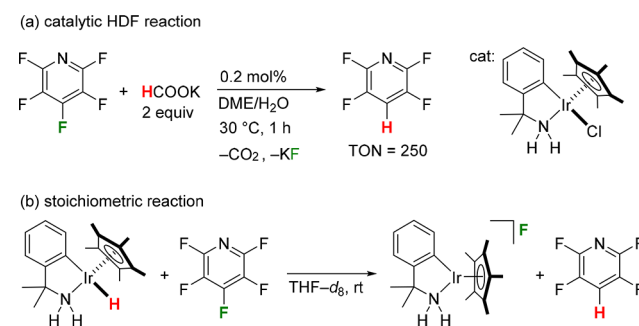


complexes subjected to a stoichiometric reaction with aromatic fluorides.^{4c,m,p,17,18} Jones proposed an S_NAr -type HDF of fluorobenzene by treatment with a hydrido-zirconium complex $[\text{Cp}^*_2\text{Zr}(\text{H})_2]$ ($\text{Cp}^* = \eta^5\text{-}1,2,3,4,5\text{-pentamethylcyclopentadienyl}$) to afford $[\text{Cp}^*_2\text{Zr}(\text{H})\text{F}]$ and benzene.¹⁶ In the Zr(IV) system, the oxidative addition mechanism could be discarded because of the lack of d-electrons on the metal. The σ -bond metathesis and S_NAr mechanisms were distinguished by comparing the reactivity of the zirconium hydride toward fluorobenzene and 1-fluoronaphthalene. The naphthalene derivative with extended conjugation was more efficiently defluorinated than fluorobenzene, likely because of the relatively stabilized structure of a transient Meisenheimer-type complex. The inverse reactivity is projected in the σ -bond metathesis mechanism, where the rate is possibly enhanced by alleviation of steric repulsion through the transition state. Therefore, σ -bond metathesis was considered to be involved in the reaction of the sterically less-hindered $[\text{Cp}_2\text{Zr}(\text{H})_2]$ with perfluorobenzene.¹⁴

While late transition metal complexes often easily cleave C–F bonds via oxidative addition,^{18i,f9} Whittlesey and co-workers have made efforts to verify the hydride-attack mechanism in the HDF of fluorinated aromatic compounds catalyzed by hydridoruthenium complexes, such as $[\text{Ru}(\text{H})_2(\text{NHC})(\text{PPh}_3)_2(\text{CO})]$, $[\text{Ru}(\text{H})_2(\text{NHC})_2(\text{PPh}_3)_2]$, and $[\text{Ru}(\text{H})_2(\text{NHC})_4]$ (NHC = *N*-heterocyclic carbene), based on computational methods.^{4p–s} Separately, nucleophilic substitution originates from an anionic metal center, which can be broadly classified into the oxidative addition mechanism, as occasionally proposed.^{18b,g}

In our transfer hydrogenation system, bifunctional iridium catalysts effectively promoted the HDF of 2,3,4,5,6-pentafluoropyridine.¹⁰ As shown in Scheme 2a, pentafluoropyridine was efficiently transformed at 30 °C using a C–N chelating iridium complex $[\text{Cp}^*\text{Ir}(\text{Cl})\{\kappa^2(\text{N},\text{C})\text{-NH}_2\text{C}(\text{CH}_3)_2\text{-}2\text{-C}_6\text{H}_4\}]$ and potassium formate to afford 2,3,5,6-tetrafluoropyridine as the sole product. The exclusive *para*-selectivity was also observed in a variety of substituted perfluorobenzenes, and the reactivity was enhanced by increasing the electron deficiency of the substrates. Coupled with these observations, the formation of the identical HDF product from an isolable coordinatively saturated hydrido-iridium complex, $[\text{Cp}^*\text{Ir}(\text{H})\{\kappa^2(\text{N},\text{C})\text{-NH}_2\text{C}(\text{CH}_3)_2\text{-}2\text{-C}_6\text{H}_4\}]$, with pentafluoropyridine (Scheme 2b) implied that the nucleophilic substitution mechanism is dominant in this catalytic HDF process.

Scheme 2. HDF of 2,3,4,5,6-Pentafluoropyridine Using Amine-Iridium Complexes



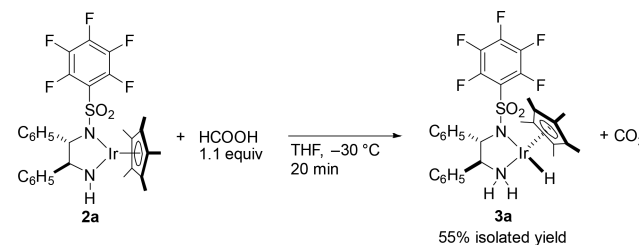
Having achieved a HDF system under transfer hydrogenation conditions, we expected that structural modification of an established bifunctional hydrido-iridium complex by introducing a fluoroaryl group onto the chelating amine framework would allow access to an intramolecular version, which will provide valuable insight into the HDF mechanism. In this paper, we explored the synthesis and chemical properties of new iridium complexes of 1,2-diphenylethylenediamine (DPEN) bearing a fluorinated phenylsulfonyl group. On the basis of the sequential process of *ortho*-selective intramolecular HDF followed by cyclometalation (C–H activation), the S_NAr mechanism involving the attack of the hydrido ligand was experimentally elucidated.

RESULTS AND DISCUSSION

Synthesis of a Hydrido-iridium Complex with *N*-Pentafluorophenylsulfonyl-1,2-diphenylethylenediamine.

According to the established procedure for synthesis of hydrido-amine complexes with *N*-sulfonyl-DPEN analogs,²⁰ a new amido-iridium complex (**2a**) derived from a chlorido-amine complex (**1a**) with a 2,3,4,5,6-pentafluorophenylsulfonyl ($\text{C}_6\text{F}_5\text{SO}_2$; Fs) group was treated with an equimolar amount of formic acid in tetrahydrofuran (THF). When the reaction was performed below -30 °C for 20 min, the desired hydrido-amine complex (**3a**) was generated in a diastereoselective manner and successfully isolated in 55% yield after removal of the solvent and washing with *n*-pentane (Scheme 3). The ^1H

Scheme 3. Synthesis of Hydrido-iridium Complex 3a from Amido Complex 2a



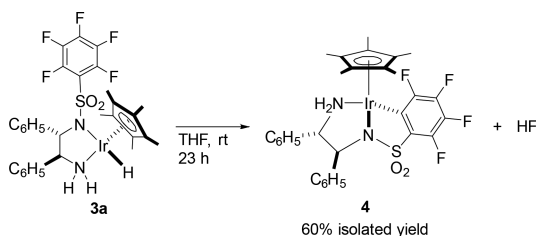
NMR spectrum of **3a** in $\text{THF-}d_8$ at -30 °C exhibited a characteristic hydrido signal at -11.00 ppm. Other signals were similar to those of **1a**. In the ^{19}F NMR spectrum, three signals attributable to the Fs moiety appeared at -132.2 , -156.1 , and -163.8 ppm with relative intensities of 2:1:2.

In contrast to preceding related hydrido-amine complexes,²¹ all manipulations of **3a**, including its isolation and NMR measurements, should be done at the low temperature due to

its thermal instability. A rapid color change from pale yellow to pink was observed at room temperature even in the solid state.

Metallacycle Formation by Thermolysis of Hydrido-iridium 3a. To shed light on the thermal decomposition of hydrido-iridium complex **3a** derived from *N*-(2,3,4,5,6-pentafluorophenylsulfonyl)-1,2-diphenylethylenediamine (FsDPEN), the complex was stirred in THF at room temperature (Scheme 4). The color of the solution changed from yellow to red-purple

Scheme 4. Spontaneous Formation of Iridacycle 4 from Hydrido Complex 3a



to finally orange over time. In the ^{19}F NMR spectrum after 23 h, no signals of **3a** were observed, and four signals appeared at -122.0 , -145.4 , -156.7 , and -163.5 ppm with equivalent intensities. These results indicated that one fluorine atom of the Fs group was liberated to afford a new species with an unsymmetrical tetrafluorophenyl unit. The ^1H NMR spectrum of the product (**4**) in CD_2Cl_2 exhibited a set of broad peaks at 3.25 and 4.01 ppm due to the NH_2 protons in proximity to the Ir center. After recrystallization from dichloromethane and diethyl ether, pale-yellow crystals of **4** were obtained in 60% yield. As illustrated in Figure 1, the structure of **4** was

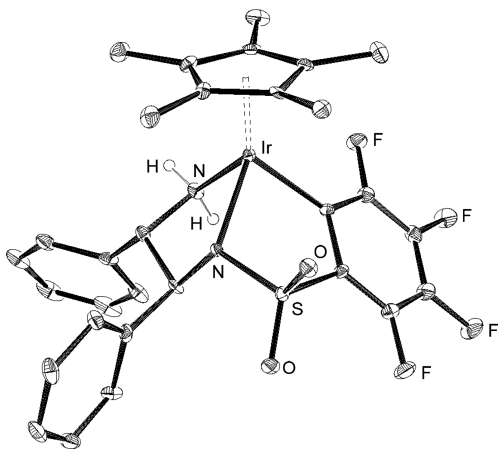


Figure 1. X-ray crystal structure of iridacycle **4**. The hydrogen atoms, except for the coordinating amine protons, are omitted for clarity. Thermal ellipsoids are shown at the 30% probability level.

determined to be an iridacycle with an orthometalated tetrafluorophenylsulfonyl moiety. The complex **4** adopts a three-legged piano-stool structure around the Ir atom attached to the Cp^* , NH_2 , sulfonylamido, and tetrafluorophenyl groups. The same iridacycle, **4**, was also directly synthesized in 89% isolated yield after mixing amido complex **2a** with an equimolar amount of formic acid in THF at room temperature for 21 h.

The progress of formation of iridacycle **4** from hydrido complex **3a** in $\text{THF-}d_8$ was monitored by ^{19}F NMR spectroscopy at room temperature. Figure 2 shows that three signals (circle) corresponding to the Fs group on **3a** gradually

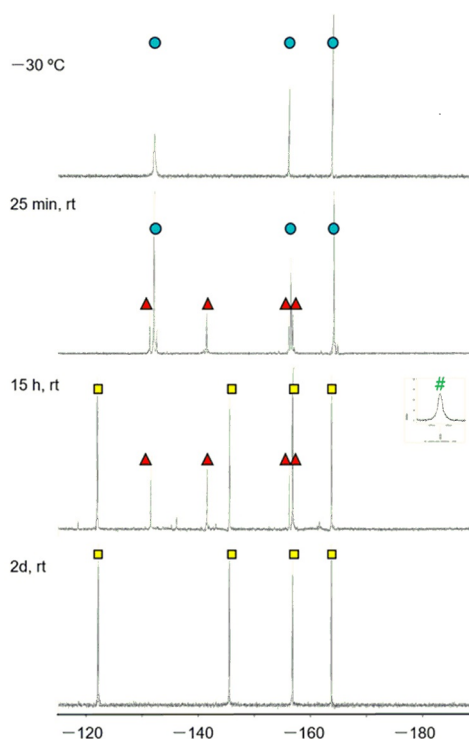


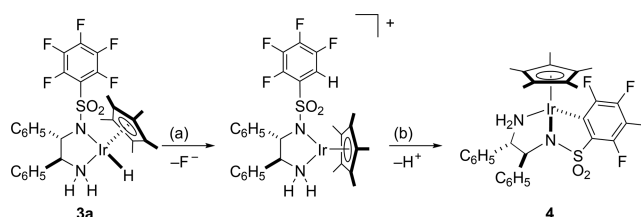
Figure 2. ^{19}F NMR monitoring of the transformation of **3a** (circle) to **4** (square) via an intermediate complex (triangle) with releasing hydrogen fluoride (#).

converted to four independent peaks (square) of resulting iridacycle **4** after 2 days. Another set of four separate signals (triangle) appeared at -131.4 , -141.4 , -156.6 , and -156.7 ppm ascribed to an intermediate in the early stage of the reaction, indicating that C–F bond cleavage took place prior to the iridacycle formation. In addition, a characteristic broad peak was also observed at -193.5 ppm (#), being indicative of a release of hydrogen fluoride.²²

Unlike our previous experimental results of intermolecular HDF showing perfect *para*-selectivity in a direct C–F bond cleavage of fluoroarenes by the related C–N chelating hydrido-iridium complex (Scheme 2b), the *ortho*-fluorine atom was substituted exclusively in this intramolecular version, where a fluorine atom near the hydrido ligand in **3a** was possibly susceptible to F/H substitution. Therefore, we postulated that iridacycle **4** was formed via a sequential mechanism including intramolecular HDF (C–F bond cleavage) and following cyclometalation (C–H bond cleavage), as shown in Scheme 5.

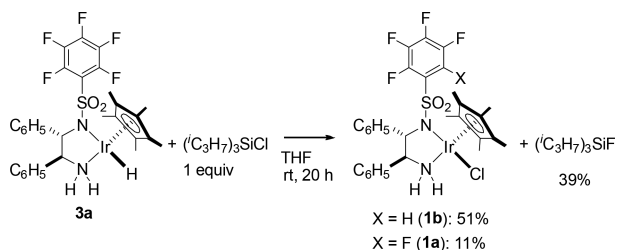
Intramolecular HDF of Hydrido-iridium 3a. To confirm the intramolecular HDF process in the proposed mechanism for the iridacycle **4** formation (step (a) in Scheme 5), we next tried to detect the liberated fluoride and an intermediary compound with a 2,3,4,5-tetrafluorophenylsulfonyl (Fs^{H}) group

Scheme 5. Sequential Formation of 4 from 3a



using chlorosilane as a fluorine-trapping reagent. When the hydrido complex **3a** was treated with triisopropylsilyl chloride in THF at room temperature for 20 h (Scheme 6), the color of

Scheme 6. Reaction of Hydrido Complex **3a** with Triisopropylsilyl Chloride at Room Temperature



the solution changed from yellow to red to finally red-orange. In the ^{19}F NMR spectrum of the resulting crude mixture, characteristic tetrafluorophenylsulfonyl signals of a new complex (**1b**) appeared at -132.5 , -141.6 , -156.2 , and -157.6 ppm, where are close to the chemical shifts of the aforementioned intermediate (triangle in Figure 2). The chlorosilane abstracted the liberated fluoride as triisopropylsilyl fluoride (39% yield), displaying a signal at -185.1 ppm,²³ while a small amount (11%) of the chloridoiridium complex bearing FsDPEN (**1a**) was also formed.

Chlorido-amine complex **1b** with the hydrodefluorinated Fs^{H} fragment was separately synthesized from *N*-(2,3,4,5-tetrafluorophenylsulfonyl)-1,2-diphenylethylenediamine ($\text{Fs}^{\text{H}}\text{DPEN}$) and $[\text{Cp}^*\text{Ir}(\mu\text{-Cl})_2]$ in 89% yield. The ^1H NMR spectrum resembled that of **1a** having FsDPEN , except for an increased integral value of the aromatic region. Orange crystals of **1b** were obtained after recrystallization from a hot methanol solution. As illustrated in Figure 3, the X-ray crystallographic structure shows a three-legged piano-stool geometry with the chelating *N*-sulfonylated DPEN ligand, similar to the structure of **1a**. The crystal structure and elemental analysis also support

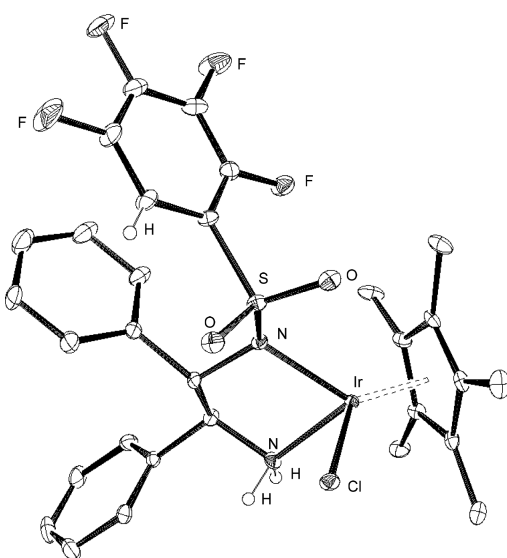
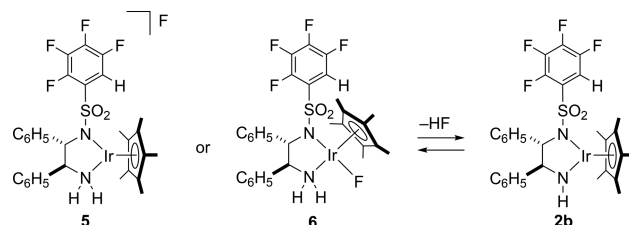


Figure 3. X-ray crystal structure of chlorido-amine complex **1b**. The hydrogen atoms, except for the coordinating amine protons and a proton on the fluoroaryl group, are omitted for clarity. Thermal ellipsoids are shown at the 30% probability level.

the structure of the *ortho*-H substitution on the fluoroarylsulfonyl moiety.

Selective C–H Cleavage on 2,3,4,5-Tetrafluorophenyl Analogs in the Cyclometalation. The HDF product possessing $\text{Fs}^{\text{H}}\text{DPEN}$ is assumed to be cyclometalated by *ortho*-selective C–H bond scission to furnish iridacycle **4** (Scheme 5b). After the HDF step (Scheme 5a), a cationic amine iridium complex (**5**) with an outer-sphere fluoride anion or a neutral aminefluoridoiridium complex (**6**),²⁴ was possibly generated, as shown in Scheme 7. Alternatively, when the

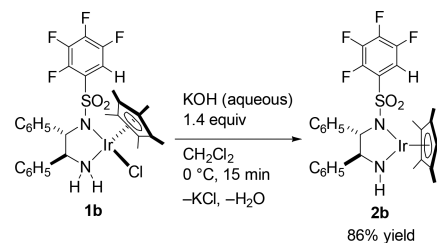
Scheme 7. Possible Transient Defluorinated Species in the Intramolecular HDF of **3a**



coordinated NH_2 was deprotonated by a basic fluoride, an amidoiridium complex (**2b**) would be formed. These three complexes might engage in the cyclometalation step.

To validate the direct cyclometalation from amido complex **2b** and a cationic amine complex, such as **5**, 16e unsaturated $\text{Fs}^{\text{H}}\text{DPEN}$ iridium complexes were prepared. Fs^{H} -amido complex **2b** was obtained in 86% yield by the reaction of isolated chlorido-amine complex **1b** with a slight excess of aqueous KOH in dichloromethane (Scheme 8). The signals in

Scheme 8. Synthesis of Amidoiridium Complex **2b**



the ^1H NMR spectrum were similar to those of analogous Fs -amido complex **2a**, except for an increase in the relative intensity of the aromatic hydrogens observed at 7.05–7.23 ppm. The four separated signals at -131.1 , -140.9 , -153.4 , and -154.2 ppm in the ^{19}F NMR spectrum in $\text{THF}-d_8$ resemble those of **1b**. The crystal structure of Fs^{H} -substituted amido complex **2b**, depicted in Figure 4, was also similar to that of Fs -analog **2a**. The phenyl groups on the DPEN framework were situated in a diaxial conformation, and a π – π stacking interaction between one of the phenyl backbones and a fluorinated phenyl group was confirmed as in the structure of **2a**.

The 16e cationic $\text{Fs}^{\text{H}}\text{DPEN}$ complex with a triflate anion (**7**) was obtained by treatment of chlorido-amine complex **1b** with a stoichiometric amount of silver triflate in dichloromethane (Scheme 9). After removal of silver chloride by filtration, recrystallization from methanol afforded red crystals of **7** in 43% yield. The chemical shift of the protons on the Cp^* ligand appeared at 1.93 ppm, which is similar to that of the corresponding amido complex **2b** at 1.95 ppm, suggesting the

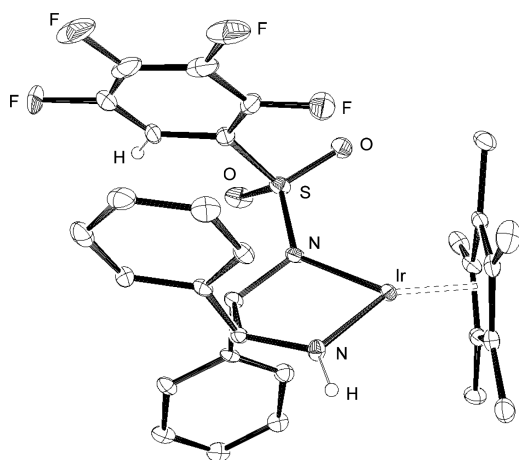
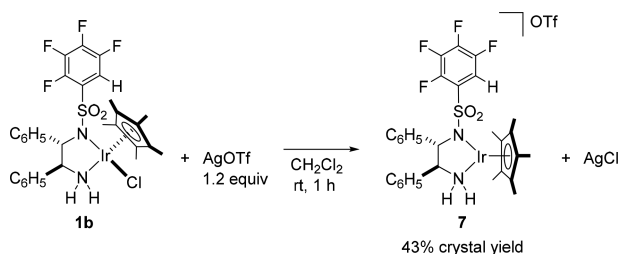


Figure 4. X-ray crystal structure of amidoiridium complex **2b**. The hydrogen atoms, except for the protons attached to the coordinating amido nitrogen and the fluoroaryl group, are omitted for clarity. Thermal ellipsoids are shown at the 30% probability level.

Scheme 9. Synthesis of Cationic Fs^H DPEN-Iridium Complex **7**

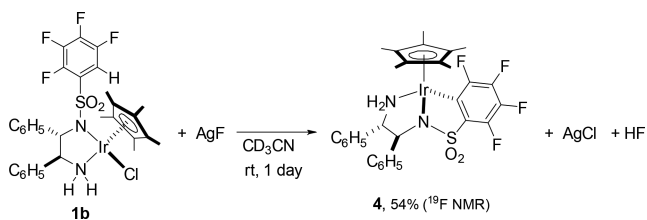


coordinatively unsaturated character of the product. Single-crystal X-ray crystallographic analysis also supported the expected planar structure (Figure S4).

The obtained 16e unsaturated complexes, amido complex **2b** and cationic complex **7**, were shown to be thermally stable in THF- d_8 at room temperature. Only 9% of iridacycle **4** was formed from amido complex **2b** even after 6 days, and cationic complex **7** remained intact in solution after 3 days. Thus, the direct C–H bond cleavage from these species is not involved in the orthometalation.

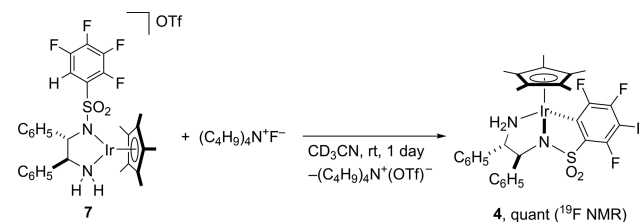
It is striking that the orthometalation efficiently proceeds in the presence of a fluoride anion. Iridacycle **4** was generated in 54% ^{19}F NMR yield after 26 h by treatment of chlorido complex **1b** with an equimolar amount of silver fluoride to perform ligand exchange in CD_3CN at room temperature (Scheme 10). Furthermore, the promoting effect of the fluoride on the cyclometalation was also clarified by treatment of cationic amine complex **7** with an equimolar amount of tetra-

Scheme 10. Reaction of Chlorido Complex **1b** and Silver Fluoride in CD_3CN at Room Temperature



butylammonium fluoride (TBAF) in CD_3CN . As shown in Scheme 11, iridacycle **4** was obtained quantitatively after 1 day.

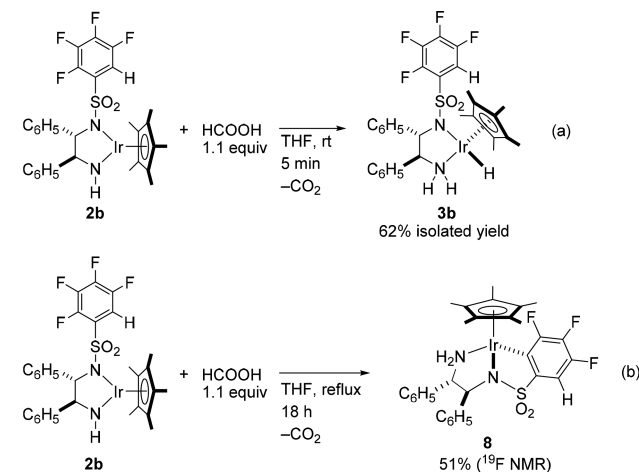
Scheme 11. Cyclometalation of Cationic Complex **7** in the Presence of TBAF



These experimental results account well for successive HDF (C–F bond cleavage) and cyclometalation (C–H bond cleavage) steps in the reaction from Fs^{H^+} DPEN-hydrido complex **3a** to iridacycle **4**. Notably, the fluoride plays an important role in the later C–H bond cleavage. Koike reported the *ortho*-selective C–H bond cleavage by alkoxido ligands on a similar amine-iridium complex bearing the TsDPEN ligand.²⁵ In a similar manner, the fluoride ligand would deprotonate the aromatic C–H bond on the Fs^H substituent with simultaneous metalation. Additionally, there are precedents for intramolecular aromatic and aliphatic C–H bond cleavage by fluoridoiridium complexes.²⁶

Synthesis and Reactivity of Hydrido-Amine Iridium Complex **3b with an Fs^H Moiety.** To illuminate the C–F bond cleavage in preference to the C–H bond, a hydridoiridium complex (**3b**) with Fs^H DPEN possessing both C–F and C–H bonds at the *ortho* positions was synthesized. As shown in Scheme 12a, **3b** was obtained in 62% isolated yield by

Scheme 12. Reaction of Fs^H DPEN-Amido Complex **2b** with a Stoichiometric Amount of Formic Acid



treatment of amido complex **2b** with a stoichiometric amount of formic acid in THF at room temperature for 5 min. The NMR spectra and crystallographic analysis of **3b** (Figure 5) verified a coordinatively saturated structure with Cp^* , NH_2 , sulfonylamido, and hydrido ligands. The hydrido ligand and amine protons were located from the Fourier map. A specific interaction between the hydrido ligand and the *ortho*-F atom on the 2,3,4,5-tetrafluorophenylsulfonyl group was not confirmed by their distance of 4.93(4) Å at this stage.

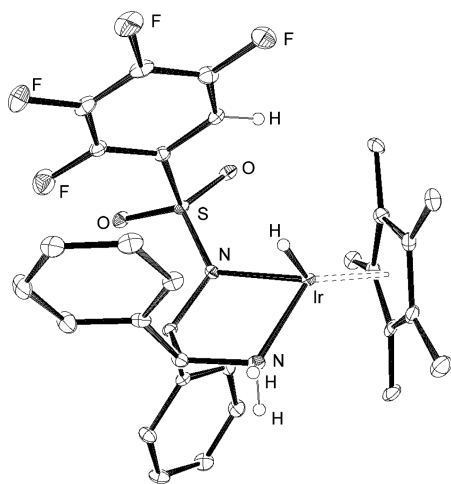


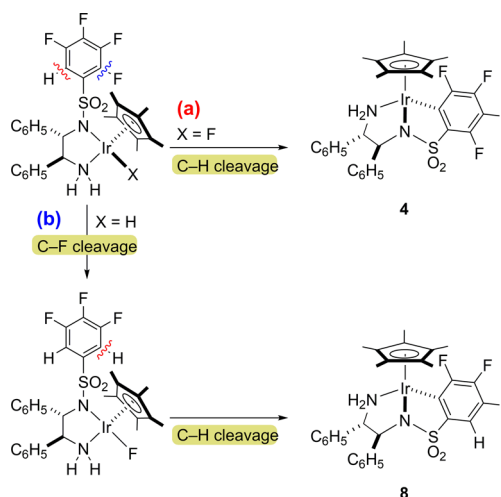
Figure 5. X-ray crystal structure of hydrido-amine complex **3b**. The hydrogen atoms, except for the hydrido ligand and the protons attached to the coordinating amine nitrogen and the fluoroaryl group, are omitted for clarity. Thermal ellipsoids are shown at the 30% probability level.

The reactivity of Fs^{H} DPEN-hydrido complex **3b** was evidently different from the corresponding Fs DPEN-hydrido complex **3a**. In contrast to the thermal instability of Fs -complex **3a** above $-30\text{ }^{\circ}\text{C}$, Fs^{H} -complex **3b** was inert at room temperature. When the reaction of Fs^{H} -substituted amidoiridium complex **2b** with an equivalent of formic acid was conducted in refluxing THF for 18 h, a new iridacycle **8** with a $\text{C}_6\text{F}_3\text{H}$ framework was formed in 51% yield (Scheme 12b). In the ^{19}F NMR spectrum in CD_2Cl_2 , three independent peaks were observed at -118.1 , -140.2 , and -158.6 ppm with equal intensities, implying the three fluorine atoms are in non-equivalent environments. After recrystallization from dichloromethane and diethyl ether, pale-yellow crystals of **8** were obtained. The structure of iridacycle **8** was quite similar to that of tetrafluoroaryl analog **4**, except for the presence of an *ortho*-H atom on the metalated fluoroaryl moiety (see Figure S4). These results underscore the generality of the iridacycle formation from the hydrido-amine iridium complexes via selective cleavage of the *ortho* C–F bonds.

Specific C–F Bond and C–H Bond Cleavage of the Fs^{H} Group. Recently, selective C–F bond and C–H bond activations of partially fluorinated aromatic compounds have received considerable attention²⁷ because of the utility of hydrofluorocarbons. Aromatic C–F and C–H bonds are often competitively activated in the oxidative addition mechanism²⁸ and thus are difficult to cleave with perfect selectivity. As mentioned above, the bifunctional Fs^{H} DPEN-iridium complexes provide access to the chemoselective cleavage of C–F and C–H bonds. The addition of fluoride to the Fs^{H} DPEN-Ir complexes (**2b** and **7**) cleanly led to the iridacycle via selective scission of the *ortho* C–H bond (cyclometalation, Scheme 13a). However, install of a hydrido ligand to the Fs^{H} DPEN-Ir complex changed the selectivity to cleave the *ortho* C–F bond (HDF), followed by cyclometalation to give $\text{C}_6\text{F}_3\text{H}$ -iridacycle **8** (Scheme 13b).

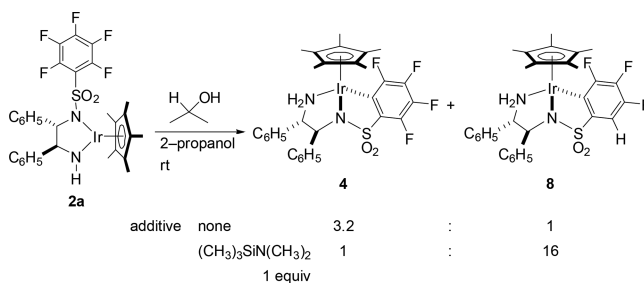
Furthermore, consecutive C–F bond scission was identified in the Fs DPEN complex. When amidoiridium complex **2a** was treated with a large excess of 2-propanol as a hydride source at room temperature for 45 h, C_6F_4 - and $\text{C}_6\text{F}_3\text{H}$ -substituted iridacycles **4** and **8** were formed in a ratio of 3.2:1, as shown in

Scheme 13. Selective Activation of the *ortho* C–F and C–H Bonds on the Amine Iridium Complexes



Scheme 14. Notably, the formation of $\text{C}_6\text{F}_3\text{H}$ -iridacycle **8** was enhanced in the presence of N,N' -dimethyltrimethylsilylamine,

Scheme 14. Treatment of Amidoiridium Complex **2a** in 2-Propanol

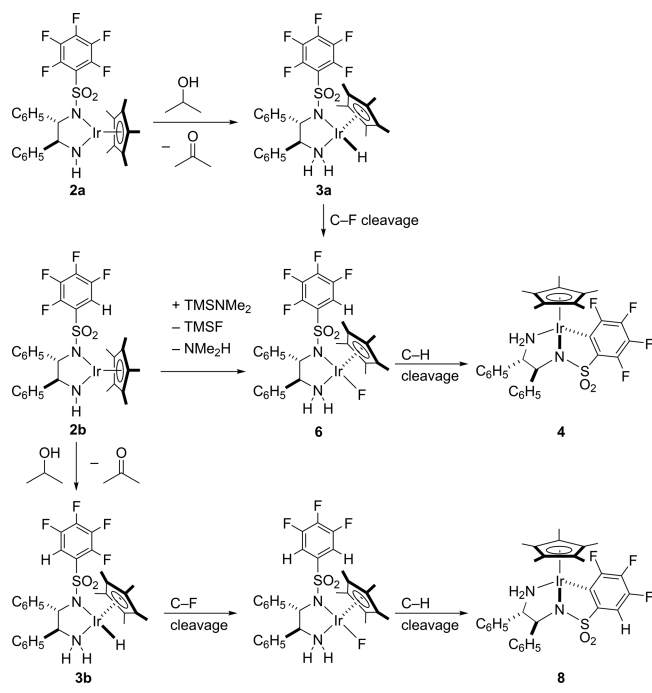


$(\text{CH}_3)_3\text{SiN}(\text{CH}_3)_2$ as a fluoride scavenger. These results could be explained by the mechanism as depicted in Scheme 15. The formation of Fs^{H} -substituted amido complex **2b** in preference to C_6F_4 -iridacycle **4** is promoted by the fluorophilic base of silylamine, possibly due to the facile abstraction of hydrogen fluoride from *in situ* generated Fs^{H} DPEN-fluoridoiridium **6**. Subsequently, Fs^{H} DPEN-hydridoiridium complex **3b** was formed from **2b** in 2-propanol and then converted to $\text{C}_6\text{F}_3\text{H}$ -iridacycle **8**.

Mechanistic Aspects of the HDF Process. For the HDF step (Schemes 5a and 13a), a set of experimental results listed below are consistent with a nucleophilic substitution mechanism and are difficult to be rationalized by other fundamental processes. (1) C–F bond cleavage (HDF) was observed only from coordinately saturated 18e hydrido-amine complexes **3a** and **3b**. (2) The C–F bond cleavage of the hydrido-amine complexes was accelerated in the electron deficient fluoroarylsulfonyl group with the increased number of the fluorine atoms (**3a** versus **3b**). (3) In the Fs^{H} DPEN-complexes, the specific cleavage of C–F or C–H bonds was achieved depending on the actor ligand: The hydrido ligand resulted in *ortho*-selective defluorinative substitution, and the fluoro ligand switched to C–H bond scission.

If the dominant mechanism for the present C–F bond activation is oxidative addition which is often reported for late transition-metal complexes, then results 1 and 3 are

Scheme 15. Plausible Mechanism for the Formation of Iridacycles **4** and **8** in 2-Propanol



inharmonious. The σ -bond metathesis of **3a** and **3b** can be unequivocally ruled out because of the coordinatively saturated nature of the hydrido-amine complexes and the conformational inaccessibility of the hydrido-iridium bond in a parallel direction to the carbon-fluorine bond at the *ortho* position, as illustrated in Figure 6a.

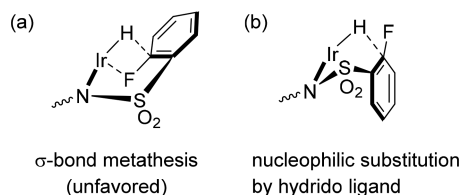


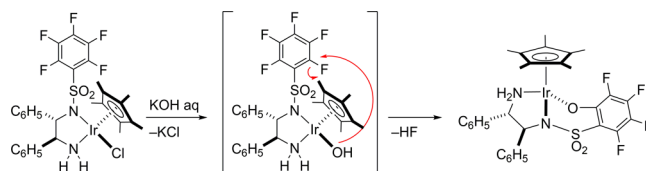
Figure 6. Postulated orientations in intramolecular C–F bond cleavage.

All observations of results 1–3 and the structural constraint (Figure 6b) accommodate the S_NAr -type HDF. The distinct reactivity between hydrido complexes **3a** and **3b** are totally consistent with the nucleophilic substitution mechanism, which should be influenced by differences in the electron deficiency of the Fs and Fs^H moieties.^{3b,10} In this context, we have already reported an intramolecular S_NAr -type substitution reaction using the related hydroxido-ruthenium and iridium complexes derived from the FsDPEN ligand (Scheme 16).²⁹ The mechanistic validity of the nucleophilic attack to the Fs group by the hydroxido ligand was supported by DFT calculations.

CONCLUSION

In summary, the fundamental steps in the HDF of aromatic fluorides was elucidated during the investigation of the reactivities of bifunctional hydrido-amine iridium complexes bearing fluorinated arylsulfonyldiamine ligands. Intramolecular *ortho*-selective C–F bond cleavage occurred using hydrido-amine complexes **3a** and **3b** bearing fluoroarylsulfonyl units.

Scheme 16. Oxametallacycle Formation via Intramolecular Nucleophilic Substitution of the FsDPEN-Ligated Hydroxidoiridium Complex



The experimental results corroborate an S_NAr -type mechanism involving nucleophilic attack by the hydride ligands, despite of the difficulty in distinguishing this pathway with σ -bond metathesis. Moreover, the successive C–H bond activation step leading to the metallacycle formation was aided by fluoride. The highly specific C–F bond and C–H bond cleavages on this family of complexes were successfully demonstrated for the first time. The findings highlighting the potential of transition-metal hydrides accessible to defluorinative aromatic substitution should strongly contribute to develop practical HDF protocols in further studies.

EXPERIMENTAL SECTION

General Procedure. All manipulations of oxygen and moisture-sensitive materials were performed under a purified argon atmosphere using standard Schlenk techniques. Solvents and formic acid were purchased from Kanto Chemical Co., Inc. and dried by refluxing over sodium benzophenone ketyl (THF and diethyl ether), P_2O_5 (CH_2Cl_2), B_2O_3 (formic acid), or CaH_2 (2-propanol), and distilled under argon before use. Deionized water was produced by a Millipore Elix system. Deuterated solvents were degassed by three freeze–pump–thaw cycles and purified by trap-to-trap distillation after being dried with CaH_2 (THF- d_8) or P_2O_5 (CD_2Cl_2 and CD_3CN). FsDPEN was prepared according to the literature method.³⁰ The other reagents were obtained from Tokyo Chemical Industry Co., Ltd., Sigma-Aldrich Co. LLC., and Wako Pure Chemical Industries Ltd., degassed, and stored under argon atmosphere. The other reagents were used as delivered. 1H (399.8 MHz), ^{19}F (376.2 MHz), and $^{13}C\{^1H\}$ (100.5 MHz) NMR were recorded on a JEOL JNM-ECX400 spectrometer at 25 °C. The NMR chemical shifts were referenced to an external tetramethylsilane signal (0.0 ppm) by using the signals of residual proton impurities in the deuterated solvents for 1H and ^{13}C , and referenced to an external CF_3CO_2H signal (–76.5 ppm) for ^{19}F NMR. Abbreviations for NMR are as follows: s = singlet, d = doublet, t = triplet, q = quartet, m = multiplet, or br = broad. Recyclable preparative high-performance liquid chromatography was performed on a Japan Analytical Industry LC-9225 NEXT system equipped with JAIGEL-1H and -2H columns using $CHCl_3$ as an eluent at a flow rate of 14 mL min^{-1} . Elemental analyses were carried out using a PE2400 Series II CHNS/O analyzer (PerkinElmer). HRMS (EI) of Fs^HCl dissolved in chloroform was analyzed by using a Double Focusing Mass Spectrometer (JEOL JMS-700).

Synthesis of (S,S)- $C_6F_4HSO_2Cl$ (Fs^HCl). To a preformed THF solution (5 mL) of 1,2,3,4-tetrafluorobenzene (1.48 g, 9.9 mmol), a hexane solution of $nBuLi$ (11.2 mmol) was added dropwise at –80 °C. Then, the obtained solution was added to a hexane solution of sulfonyl chloride at –80 °C. After stirring the mixture for 12 h from –80 to 0 °C, the solution was washed with water, then purified by a preparative gel permeation chromatography (GPC) to give $C_6F_4HSO_2Cl$ (718 mg, 2.89 mmol) as a pale yellow oil. 29% yield. 1H NMR ($CDCl_3$, r.t., δ/ppm): 7.70 (m, 1H). ^{19}F NMR ($CDCl_3$, r.t., δ/ppm): –148.3 (dd, $^3J_{FF} = 20$ Hz, 1 F), –140.2 (m, 1F), –133.4 (m, 1F), –130.9 (m, 1F). $^{13}C\{^1H\}$ NMR ($CDCl_3$, r.t., δ/ppm): 111.5 (d $^2J_{CF} = 22$ Hz, $C_{FsHippo}$), 128.0 ($HC_{FsHortho}$), 141.7 (dt, $^1J_{CF} = 261.7$ Hz, $^2J_{CF} = 13$ –16 Hz), 145.3 (dd, $^1J_{CF} = 264$ Hz, $^2J_{CF} = 12$ –15 Hz), 145.9 (dd, $^1J_{CF} = 267.4$ Hz), 146.3 (dd, $^1J_{CF} = 256$ Hz, $^2J_{CF} = 9$ –11 Hz). HRMS (EI) Calcd for $C_6HClF_4O_2S$: 247.9322, Found: 247.9321.

Synthesis of (S,S)-C₆F₄HSO₂NHCHPhCHPhNH₂ (Fs^HDPEN). To a preformed CH₂Cl₂ (30 mL) solution of (S,S)-DPEN (332 mg, 1.57 mmol) and trimethylamine (204 mg, 2.01 mmol), a CH₂Cl₂ (10 mL) solution of Fs^HCl (387 mg, 1.57 mmol) was added dropwise at 0 °C and stirred for 7 h. After washing with water (20 mL × 3), the organic layer was dried over Na₂SO₄, and the solvent was then removed under reduced pressure. The residue was purified by column chromatography on silica gel eluting with hexane/ethyl acetate (10:1 to 1:1) to afford the desired product of Fs^HDPEN as a white powder in 72% yield (474 mg, 1.12 mmol). ¹H NMR (CDCl₃, r.t., δ/ppm): 4.28 (d ³J_{HH} = 3.9 Hz, Fs^HCH(C₆H₅)NHCH(C₆H₅)NH₂, 1H), 4.46 (d ³J_{HH} = 3.7 Hz, Fs^HCH(C₆H₅)NHCH(C₆H₅)NH₂, 1H), 7.11–7.27 (m, aryl, 7H), 7.31–7.32 (m, aryl, 4H). ¹⁹F NMR (CDCl₃, r.t., δ/ppm): –151.1 (apparent dd, 1F), –147.9 (m, 1F), –137.1 (m, 1F), –132.4 (m, 1F). ¹³C{¹H} NMR (CDCl₃, r.t., δ/ppm): 59.6 (Fs^HNHCHPhCHPhNH₂), 63.4 (Fs^HNHCHPhCHPhNH₂), 111.3 (dd ²J_{CF} = 22 Hz, ³J_{CF} = 2.8 Hz, C_{FsHippo}), 124.7 (HC_{FsOrtho}), 126.1, 126.4, 127.6, 127.8, 128.3, 128.6, 139.1, 140.8, 140.5 (dt, ¹J_{CF} = 236 Hz, ²J_{CF} = 14 Hz), 143.0 (dt, ¹J_{CF} = 235 Hz), 143.9 (dd, ¹J_{CF} = 267 Hz, ²J_{CF} = 11 Hz), 145.7 (dd, ¹J_{CF} = 262 Hz, ²J_{CF} = 12 Hz). Anal. Calcd for [C₂₀H₁₆F₄N₂O₂S]: C, 56.60; H, 3.80; N, 6.60. Found: C, 56.33; H, 3.78; N, 6.48%.

Synthesis of Cp*IrCl[κ²(N,N')-(S,S)-C₆F₅SO₂NCHPhCHPhNH₂] (1a). A mixture of [Cp*IrCl(μ-Cl)]₂ (853.5 mg, 1.07 mmol), FsDPEN (947.8 mg, 2.14 mmol), and aqueous KOH (120.1 mg, 2.14 mmol in 5 mL of water) in CH₂Cl₂ (40 mL) was stirred at room temperature for 17 h. The obtained yellow organic layer was washed with water, dried over Na₂SO₄, and subsequently evaporated to dryness to afford a bright yellow powder. After recrystallization by slow diffusion of Et₂O into a CH₂Cl₂ solution, yellow crystals of 1a were isolated in 81% yield (1.391 g, 1.73 mmol). Further recrystallization from hot methanol gave yellow needle crystals suitable for X-ray crystallography (Figure S2). ¹H NMR (CD₂Cl₂, r.t., δ/ppm): 1.74 (s, C₅(CH₃)₅, 15H), 3.72 (t ³J_{HH} = 11 Hz, C₆F₅SO₂NCHPhCHPhNH₂, 1H), 4.20 (br d ³J_{HH} = 10 Hz, C₆F₅SO₂NCHPhCHPhNH₂, 1H), 4.43 (vt ³J_{HH} = 10 Hz ³J_{HH} = 14 Hz, C₆F₅SO₂NCHPhCHPhNH₂, 1H), 4.61 (d ³J_{HH} = 11 Hz, C₆F₅SO₂NCHPhCHPhNH₂, 1H), 6.89–6.97 (m, aryl, 7H), 7.17–7.21 (m, aryl, 3H). ¹H NMR (THF-d₈, r.t., δ/ppm): 1.74 (s, C₅(CH₃)₅, 15H), 3.64 (vt ³J_{HH} = 11 Hz ³J_{HH} = 17 Hz, C₆F₅SO₂NCHPhCHPhNH₂, 1H), 4.26 (vt ³J_{HH} = 12 Hz ³J_{HH} = 13 Hz, C₆F₅SO₂NCHPhCHPhNH₂, 1H), 4.67 (d ³J_{HH} = 10 Hz, C₆F₅SO₂NCHPhCHPhNH₂, 1H), 5.78 (br d ³J_{HH} = 10 Hz, C₆F₅SO₂NCHPhCHPhNH₂, 1H), 4.61 (d ³J_{HH} = 11 Hz, C₆F₅SO₂NCHPhCHPhNH₂, 1H), 6.89–6.97 (m, aryl, 7H), 7.17–7.21 (m, aryl, 3H). ¹⁹F NMR (CD₂Cl₂, r.t., δ/ppm): –162.7 (apparent t, meta-F, 2F), –153.2 (apparent dd, para-F, 1F), –133.7 (apparent d, ortho-F, 2F). ¹⁹F NMR (THF-d₈, r.t., δ/ppm): –164.7 (meta-F, 2F), –156.8 (para-F, 1F), –133.3 (ortho-F, 2F). ¹³C{¹H} NMR (CD₂Cl₂, r.t., δ/ppm): 9.20 (C₅(CH₃)₅), 68.4 (C₆F₅SO₂NCHPhCHPhNH₂), 73.3 (C₆F₅SO₂NCHPhCHPhNH₂), 86.3 (C₅(CH₃)₅), 121.9 (t ²J_{CF} = 14.4 Hz, C_{Fsippo} 1C), 127.1 (Ph, 1C), 127.2 (Ph, 2C), 127.4 (Ph, 2C), 128.1 (Ph, 2C), 128.9 (Ph, 3C), 137.0 (C_{Fsmeta} 2C), 138.2 (C_{Phippo} 1C), 139.3 (C_{Phippo} 1C), 141.5 (C_{Fsparat} 1C), 144.1 (dd ¹J_{CF} = 257 Hz, C_{Fortho} 2C). Anal. Calcd for C₃₀H₂₉ClF₅IrN₂O₂S: C, 44.80; H, 3.63; N, 3.48. Found: C, 44.46; H, 3.59; N, 3.30.

Synthesis of Cp*Ir[κ²(N,N')-(S,S)-C₆F₅SO₂NCHPhCHPhNH₂] (2a). A KOH (128.9 mg, 2.30 mmol) solution in 5 mL of water was added to 1a (1.385 g, 1.72 mmol) in CH₂Cl₂ (40 mL) at room temperature. After stirring at room temperature for 15 min, the purple organic layer was washed with water (3 mL × 3), dried over Na₂SO₄, and further dried using CaH₂. After filtration by Celite, the dehydrated filtrate was evaporated to dryness to afford 2a as a red-purple solid (1.197 g, 1.56 mmol) in 91% yield. Recrystallization from Et₂O gave red-purple crystals suitable for X-ray crystallography (Figure S3). ¹H NMR (CD₂Cl₂, r.t., δ/ppm): 1.95 (s, C₅(CH₃)₅, 15H), 4.03 (s, C₆F₅SO₂NCHPhCHPhNH₂, 1H), 4.06 (d ³J_{HH} = 4.2 Hz, C₆F₅SO₂NCHPhCHPhNH₂, 1H), 5.39 (br, C₆F₅SO₂NCHPhCHPhNH₂, 1H), 6.97–7.07 (m, aryl, 1H), 7.10–7.15 (m, aryl, 4H), 7.21–7.25 (m, aryl, 1H), 7.29–7.33 (t, aryl, 2H), 7.56–7.58 (d, aryl, 2H). ¹H NMR (THF-d₈, r.t., δ/ppm): 1.96 (s, C₅(CH₃)₅, 15H), 4.00 (d, C₆F₅SO₂NCHPhCHPhNH₂, 1H), 4.09 (s, P

C₆F₅SO₂NCHPhCHPhNH₂, 1H), 6.18 (br, C₆F₅SO₂NCHPhCHPhNH₂, 1H), 6.97–7.23 (m, aryl, 8H), 7.58 (d, aryl, 2H). ¹⁹F NMR (CD₂Cl₂, r.t., δ/ppm): –160.6 (apparent t, meta-F, 2F), –151.7 (apparent t, para-F, 1F), –134.2 (apparent d, ortho-F, 2F). ¹⁹F NMR (THF-d₈, r.t., δ/ppm): –163.5 (m, meta-F, 2F), –155.4 (m, para-F, 1F), –135.6 (m, ortho-F, 2F). ¹³C{¹H} NMR (CD₂Cl₂, r.t., δ/ppm): 10.1 (C₅(CH₃)₅), 72.9 79.1 (C₆F₅SO₂NCHPhCHPhNH₂), 85.9 (C₅(CH₃)₅), 117.7 (C_{Fsippo} 1C), 126.0 (Ph, 2C), 126.5 (Ph, 1C), 126.7 (Ph, 1C), 127.1 (Ph, 2C), 127.6 (Ph, 4C), 136.9 (C_{Fsmeta} 2C), 141.7 (C_{Fsparat} 1C), 143.8 (C_{Fortho} 2C), 144.7 (C_{Phippo} 1C), 147.2 (C_{Phippo} 1C). Anal. Calcd for C₃₁H₃₀Cl₂F₅IrN₂O₂S: C, 43.66; H, 3.55; N, 3.29. Found: C, 43.71; H, 3.39; N, 3.37.

Synthesis of Cp*Ir(H)[κ²(N,N')-(S,S)-C₆F₅SO₂NCHPhCHPhNH₂] (3a). Formic acid (9.5 mg, 0.21 mmol) was added to a THF (10 mL) solution of 2a (153.7 mg, 0.200 mmol) at –30 °C. The readily formed yellow solution was stirred for 20 min below –30 °C, and the solvent was removed under reduced pressure. The resulting pale-yellow powder was washed with cold Et₂O (3 mL × 2) and dried in vacuo to give 3a in 55% isolated yield (84.6 mg, 0.110 mmol). All the manipulations must be performed under –30 °C because 3a is thermally unstable and converts to iridacycle complex 4. ¹H NMR (THF-d₈, –30 °C, δ/ppm): –11.4 (br, IrH, 1H), 1.87 (s, C₅(CH₃)₅, 15H), 3.59 (overlapped with THF, C₆F₅SO₂NCHPhCHPhNH₂, 1H), 4.43 (d ³J_{HH} = 9.2 Hz, C₆F₅SO₂NCHPhCHPhNH₂, 1H), 5.18 (d ³J_{HH} = 8.5 Hz, C₆F₅SO₂NCHPhCHPhNH₂, 1H), 5.61 (dd ³J_{HH} = 10.5, 11.3 Hz, C₆F₅SO₂NCHPhCHPhNH₂, 1H), 6.96–7.02 (br, aryl, 7H), 7.14 (br, aryl, 3H). ¹⁹F NMR (THF-d₈, r.t., δ/ppm): –163.8 (apparent t, meta-F, 2F), –156.1 (apparent t, para-F, 1F), –132.2 (br, ortho-F, 2F). ¹³C{¹H} NMR (THF-d₈, r.t., δ/ppm): 10.9 (C₅(CH₃)₅), 71.9 (C₆F₅SO₂NCHPhCHPhNH₂), 76.7 (C₆F₅SO₂NCHPhCHPhNH₂), 87.7 (C₅(CH₃)₅), 121.9, 127.5, 128.7, 129.1, 129.2, 129.6, 137.1, 139.8, 142.0, 144.4, 146.9.

Synthesis of Cp*Ir[κ²(N,N',C)-(S,S)-C₆F₄SO₂NCHPhCHPhNH₂] (4). **Method A.** Formic acid (9.2 mg, 0.20 mmol) was added to a THF (10 mL) solution of 2a (153.8 mg, 0.20 mmol) at room temperature. A gradual color change of the reaction mixture from yellow to purplish red and then to orange indicated the formation of 4. After stirring for 21 h, the solvent was removed under reduced pressure. The resulting dark orange solid was washed with hexane (3 mL × 3) and dried in vacuo. The isolated yield was 89% (133.5 mg, 0.18 mmol). Yellow crystals suitable for X-ray crystallography were successfully obtained after recrystallization by slow diffusion of Et₂O into a CH₂Cl₂ solution.

Method B. Separately, 4 (43.8 mg, 0.058 mmol) was obtained in 60% yield from a THF (5 mL) solution of isolated hydrido complex 3a (74.5 mg, 9.68 × 10^{–2} mmol), after stirring for 23 h at room temperature. ¹H NMR (CD₂Cl₂, r.t., δ/ppm): 1.79 (s, C₅(CH₃)₅, 15H), 3.25 (br dd ³J_{HH} = 12, 12.7 Hz, ArSO₂NCHPhCHPhNH₂, 1H), 3.58 (ddd ³J_{HH} = 13.6 Hz ⁴J_{HH} = 2.8 Hz, ArSO₂NCHPhCHPhNH₂, 1H), 3.95 (d ³J_{HH} = 10.9 Hz, ArSO₂NCHPhCHPhNH₂, 1H), 4.01 (d ³J_{HH} = 10.2 Hz, ArSO₂NCHPhCHPhNH₂, 1H), 6.83 (d ³J_{HH} = 7.8 Hz, aryl, 2H), 7.03–7.13 (m, aryl, 5H), 7.18–7.26 (m, aryl, 3H). ¹H NMR (THF-d₈, r.t., δ/ppm): 1.81 (s, C₅(CH₃)₅, 15H), 3.55 (overlapped, confirmed by the COSY spectrum, ArSO₂NCHPhCHPhNH₂, 1H), 3.95 (br t ³J_{HH} = 11 Hz, ArSO₂NCHPhCHPhNH₂, 1H), 3.96 (d ³J_{HH} = 11 Hz, ArSO₂NCHPhCHPhNH₂, 1H), 5.48 (br d ³J_{HH} = 9.9 Hz, 1H), 6.89–7.11 (m, aryl, 10H). ¹⁹F NMR (CD₂Cl₂, r.t., δ/ppm): –160.3 (apparent dd, F^a, 1F), –153.3 (apparent ddd, F^b, 1F), –144.1 (apparent ddd, F^a, 1F), –121.8 (apparent dd, F^d, 1F). ¹⁹F NMR (THF-d₈, r.t., δ/ppm): –163.5 (apparent dd, F^b, 1F), –156.7 (apparent dd, 1F), –145.4 (apparent t, F^a, 1F), –122.0 (apparent dd, F^d, 1F). ¹³C{¹H} NMR (CD₂Cl₂, r.t., δ/ppm): 8.98 (s, C₅(CH₃)₅), 69.6 (s, ArSO₂NCHPhCHPhNH₂), 75.3 (s, ArSO₂NCHPhCHPhNH₂), 88.7 (s, C₅(CH₃)₅), 125.4 (C_{C₆F₄} 1C), 126.9, 127.8, 129.0 (Ph, 10C), 130 (C_{C₆F₄} 1C), 138.0 (C_{C₆F₄} 1C), 138.1 (C_{Phippo} 1C), 142.1 (C_{Phippo} 1C), 143.9 (C_{Ph} 1C), 148.7 (C_{C₆F₄} 1C). Anal. Calcd for C₃₀H₂₉F₄IrN₂O₂S: C, 48.05; H, 3.90; N, 3.74. Found: C, 48.26; H, 3.88; N, 3.63.

Synthesis of $\text{Cp}^*\text{IrCl}[\kappa^2(\text{N}, \text{N}')-(\text{S}, \text{S})-\text{C}_6\text{F}_4\text{HSO}_2\text{NCHPhCHPhNH}_2]$ (1b**).** A mixture of $[(\eta^5\text{-C}_5\text{Me}_5)\text{IrCl}(\mu\text{-Cl})_2]$ (877.0 mg, 1.10 mmol), $\text{Fs}^{\text{H}}\text{DPEN}$ (934.1 mg, 2.20 mmol), and aqueous KOH (140.8 mg, 2.51 mmol in 2 mL of water) in CH_2Cl_2 (25 mL) was stirred at room temperature for 4 h. The resulting yellow organic layer was washed with water (2 mL \times 5), dried over Na_2SO_4 , and subsequently evaporated to dryness to afford a bright yellow powder of **1b**. Recrystallization from hot methanol gave orange crystals in 89% isolated yield (1.524 g, 1.95 mmol). ^1H NMR (CD_2Cl_2 , r.t., δ /ppm): 1.75 (s, $\text{C}_5(\text{CH}_3)_5$, 15H), 3.73 (ddd $^3J_{\text{HH}} = 13$ Hz $^3J_{\text{HH}} = 11$ Hz $^3J_{\text{HH}} = 3.0$ Hz, $\text{C}_6\text{F}_4\text{HSO}_2\text{NCHPhCHPhNH}_2$, 1H), 4.23 (d $^3J_{\text{HH}} = 10.0$ Hz, $\text{C}_6\text{F}_4\text{HSO}_2\text{NCHPhCHPhNH}_2$, 1H), 4.45 (br d $^3J_{\text{HH}} = 12$ Hz, $\text{C}_6\text{F}_4\text{HSO}_2\text{NCHPhCHPhNH}_2$, 1H), 4.48 (d $^3J_{\text{HH}} = 11$ Hz, $\text{C}_6\text{F}_4\text{HSO}_2\text{NCHPhCHPhNH}_2$, 1H), 6.80–6.81 (m, aryl, 2H), 6.84–6.87 (m, aryl, 3H), 6.95–6.97 (m, aryl, 2H), 7.15–7.19 (m, aryl, 3H). ^{19}F NMR (CD_2Cl_2 , r.t., δ /ppm): –155.8 (apparent t, 1F), –153.1 (m, 1F), –139.8 (m, 1F), –132.5 (m, 1F). These peaks were characterized based on homodecoupling experiments (Figure S1). $^{13}\text{C}\{^1\text{H}\}$ NMR (CD_2Cl_2 , r.t., δ /ppm): 9.26 ($\text{C}_5(\text{CH}_3)_5$), 68.7 ($\text{C}_6\text{F}_4\text{HSO}_2\text{NCHPhCHPhNH}_2$), 73.2 ($\text{C}_6\text{F}_4\text{HSO}_2\text{NCHPhCHPhNH}_2$), 86.1 ($\text{C}_5(\text{CH}_3)_5$), 113.1 (d, $^2J_{\text{CF}} = 22$ Hz, $\text{C}_{\text{C}_6\text{F}_4\text{H}_{\text{ipso}}}$ 1C), 127.1, 127.2, 127.4, 128.5, 128.8, 130.3 (t $^2J_{\text{CF}} = 15.3$ Hz, $\text{C}_{\text{C}_6\text{F}_4\text{ortho(H)}}$ 1C), 138.3 ($\text{C}_{\text{Ph}_{\text{ipso}}}$), 138.7 ($\text{C}_{\text{Ph}_{\text{ipso}}}$), 142.3 (t, $^2J_{\text{CF}} = 13.4$ Hz, $\text{C}_{\text{C}_6\text{F}_4}$ 1C), 143.7 (d, $^2J_{\text{CF}} = 10.6$ Hz, $\text{C}_{\text{C}_6\text{F}_4\text{H}}$ 1C), 144.7 (m, $^2J_{\text{CF}} = 10.6$ Hz, $\text{C}_{\text{C}_6\text{F}_4\text{H}}$ 1C), 146.1 (d, $^2J_{\text{CF}} = 12.5$ Hz, $\text{C}_{\text{C}_6\text{F}_4\text{H}}$ 1C). Anal. Calcd for $\text{C}_{30}\text{H}_{30}\text{ClF}_4\text{IrN}_2\text{O}_2\text{S}$: C, 45.82; H, 3.85; N, 3.56. Found: C, 45.90; H, 3.81; N, 3.65.

Synthesis of $\text{Cp}^*\text{Ir}[\kappa^2(\text{N}, \text{N}')-(\text{S}, \text{S})-\text{C}_6\text{F}_4\text{HSO}_2\text{NCHPhCHPhNH}]$ (2b**).** A KOH (40.3 mg, 0.718 mmol) solution in 2 mL of water was added to **1b** (393.2 mg, 0.50 mmol) in CH_2Cl_2 (15 mL) at 0 °C. After stirring at room temperature for 15 min, the purple organic layer was washed with water (2 mL \times 5), dried over Na_2SO_4 , and further dried using CaH_2 . After filtration by Celite, the dehydrated filtrate was evaporated to dryness to afford a red-purple solid of **2b** in 86% yield (320.7 mg, 1.56 mmol). ^1H NMR (CD_2Cl_2 , r.t., δ /ppm): 1.95 (s, $\text{C}_5(\text{CH}_3)_5$, 15H), 3.94 (s, $\text{C}_6\text{F}_4\text{HSO}_2\text{NCHPhCHPhNH}$, 1H), 4.04 (d $^3J_{\text{HH}} = 4.6$ Hz, $\text{C}_6\text{F}_4\text{HSO}_2\text{NCHPhCHPhNH}$, 1H), 5.37 (br, $\text{C}_6\text{F}_4\text{HSO}_2\text{NCHPhCHPhNH}$, 1H), 7.05–7.16 (m, aryl, 6H), 7.19–7.23 (m, aryl, 1H), 7.21 (m, aryl, 1H), 7.30 (m, 2H; aryl), 7.55 (d $^3J_{\text{HH}} = 7.3$ Hz, 2H; aryl). ^1H NMR (THF- d_6 , r.t., δ /ppm): 1.96 (s, $\text{C}_5(\text{CH}_3)_5$, 15H), 3.98 (overlapped, $\text{C}_6\text{F}_4\text{HSO}_2\text{NCHPhCHPhNH}$ and $\text{C}_6\text{F}_4\text{HSO}_2\text{NCHPhCHPhNH}$, 2H), 6.13 (br, $\text{C}_6\text{F}_4\text{HSO}_2\text{NCHPhCHPhNH}$, 1H), 6.99–7.21 (m, aryl, 9H), 7.55 (d $^3J_{\text{HH}} = 7.7$ Hz, aryl, 1H). ^{19}F NMR (CD_2Cl_2 , r.t., δ /ppm): –151.9 (m, 1F), –151.7 (apparent t, 1F), –139.4 (m, 1F), –130.6 (m, 1F). ^{19}F NMR (THF- d_6 , r.t., δ /ppm): –154.2 (m, 1F), –153.4 (apparent t, 1F), –140.9 (m, 1F), –131.1 (m, 1F). $^{13}\text{C}\{^1\text{H}\}$ NMR (CD_2Cl_2 , r.t., δ /ppm): 10.1 ($\text{C}_5(\text{CH}_3)_5$), 73.2 ($\text{C}_6\text{F}_4\text{HSO}_2\text{NCHPhCHPhNH}$), 79.3 ($\text{C}_6\text{F}_4\text{HSO}_2\text{NCHPhCHPhNH}$), 85.8 ($\text{C}_5(\text{CH}_3)_5$), 111.5 (d $^2J_{\text{CF}} = 21$ Hz, $\text{C}_{\text{C}_6\text{F}_4\text{H-CH}}$ 1C), 126.1 (Ph, 2C), 126.6 (Ph, 2C), 127.1 (Ph, 2C), 127.6 (Ph, 4C), 140.3 ($\text{C}_{\text{C}_6\text{F}_4\text{H}}$ 2C), 141.5 ($\text{C}_{\text{C}_6\text{F}_4\text{H}}$ 2C), 145.1 (dd $^1J_{\text{CF}} = 249.2$ Hz $^2J_{\text{CF}} = 9.6$ Hz, $\text{C}_{\text{C}_6\text{F}_4\text{H}}$ 2C), 145.3 ($\text{C}_{\text{Ph}_{\text{ipso}}}$ 1C), 146.8 ($\text{C}_{\text{Ph}_{\text{ipso}}}$ 1C). Anal. Calcd for $\text{C}_{30}\text{H}_{29}\text{F}_4\text{IrN}_2\text{O}_2\text{S}$: C, 48.05; H, 3.90; N, 3.74. Found: C, 47.84; H, 4.05; N, 3.62.

Synthesis of $\text{Cp}^*\text{Ir}(\text{H})[\kappa^2(\text{N}, \text{N}')-(\text{S}, \text{S})-\text{C}_6\text{F}_4\text{HSO}_2\text{NCHPhCHPhNH}_2]$ (3b**).** Formic acid (6.6 mg, 0.143 mmol) was added to a THF (6.5 mL) solution of **2b** (100.7 mg, 0.134 mmol) at room temperature. The readily formed yellow solution was stirred for 5 min, and the solvent was removed under reduced pressure. The resulting pale-yellow powder was washed with hexane (2.5 mL \times 3) and dried in vacuo to give **3b** in 62% isolated yield (62.3 mg, 8.29×10^{-2} mmol). Recrystallization from methanol gave pale-yellow crystals. ^1H NMR (THF- d_6 , 0 °C, δ /ppm): –10.9 (br, IrH, 1H), 1.87 (s, $\text{C}_5(\text{CH}_3)_5$, 15H), 3.63 (m, $\text{C}_6\text{F}_4\text{HSO}_2\text{NCHPhCHPhNH}_2$, 1H), 4.35 (d $^3J_{\text{HH}} = 9.5$ Hz, $\text{C}_6\text{F}_4\text{HSO}_2\text{NCHPhCHPhNH}_2$, 1H), 5.02 (br d $^3J_{\text{HH}} = 9.9$ Hz, $\text{C}_6\text{F}_4\text{HSO}_2\text{NCHPhCHPhNH}_2$, 1H), 5.48 (br dd $^3J_{\text{HH}} = 11, 12$ Hz, $\text{C}_6\text{F}_4\text{HSO}_2\text{NCHPhCHPhNH}_2$, 1H), 6.92–7.00 (m, aryl, 7H), 7.11–

7.13 (m, aryl, 3H), 7.37 (m, aryl, 1H). ^{19}F NMR (THF- d_6 , 40 °C, δ /ppm): –156.8 (1F), –156.1 (1F), –141.4 (1F), –131.5 (1F); Anal. Calcd for $\text{C}_{30}\text{H}_{31}\text{F}_4\text{IrN}_2\text{O}_2\text{S}$: C, 47.93; H, 4.16; N, 3.73. Found: C, 47.92; H, 4.32; N, 3.69.

Synthesis of $[\text{Cp}^*\text{Ir}\{\kappa^2(\text{N}, \text{N}')-(\text{S}, \text{S})-\text{C}_6\text{F}_4\text{HSO}_2\text{NCHPhCHPhNH}_2\}^+(\text{OTf})^-]$ (7**).** A solution of **1b** (157.8 mg, 0.20 mmol) and silver triflate (61.9 mg, 0.241 mmol) in CH_2Cl_2 (10 mL) was stirred for 1 h. The resulting red solution was filtered through Celite, and the solvent was removed under reduced pressure. Recrystallization of the resulting red powder from methanol gave red crystals of **7** in 43% yield (76.9 mg, 8.55×10^{-2} mmol, 43%). ^1H NMR (CD_2Cl_2 , rt, δ /ppm): 1.87 (s, $\text{C}_5(\text{CH}_3)_5$, 15H), 4.35 (d $^3J_{\text{HH}} = 4.5$ Hz, $\text{C}_6\text{F}_4\text{HSO}_2\text{NCHPhCHPhNH}_2$, 1H), 5.18 (br d $^3J_{\text{HH}} = 9.7$ Hz, $\text{C}_6\text{F}_4\text{HSO}_2\text{NCHPhCHPhNH}_2$, 1H), 6.08 (d $^3J_{\text{HH}} = 13$ Hz, $\text{C}_6\text{F}_4\text{HSO}_2\text{NCHPhCHPhNH}_2$, 1H), 7.09–7.11 (m, aryl, 2H), 7.13–7.15 (m, aryl, 2H), 7.19–7.29 (m, aryl, 5H), 7.30–7.36 (m, aryl, 2H). ^1H NMR (THF- d_6 , rt, δ /ppm): 1.93 (s, $\text{C}_5(\text{CH}_3)_5$, 15H), 4.37 (dd $^3J_{\text{HH}} = 2.4, 2.5$ Hz, $\text{C}_6\text{F}_4\text{HSO}_2\text{NCHPhCHPhNH}_2$, 1H), 4.60 (d $^3J_{\text{HH}} = 1.8$ Hz, $\text{C}_6\text{F}_4\text{HSO}_2\text{NCHPhCHPhNH}_2$, 1H), 6.31 (br d $^3J_{\text{HH}} = 13$ Hz, $\text{C}_6\text{F}_4\text{HSO}_2\text{NCHPhCHPhNH}_2$, 1H), 6.72 (br d $^3J_{\text{HH}} = 12$ Hz, $\text{C}_6\text{F}_4\text{HSO}_2\text{NCHPhCHPhNH}_2$, 1H), 7.15–7.20 (m, aryl, 6H), 7.25–7.26 (m, aryl, 5H). ^{19}F NMR (CD_2Cl_2 , r.t., δ /ppm): –150.0 (apparent dd, 1F), –146.9 (br s, 1F), –136.6 (br s, 1F), –130.0 (br s, 1F), –77.8 (s, 3F; OSO_2CF_3). ^{19}F NMR (THF- d_6 , r.t., δ /ppm): –151.9 (t $^3J_{\text{FF}} = 23, 20$ Hz, 1F), –150.1 (m, 1F), –138.8 (m, 1F), –130.7 (m, 1F), –78.0 (s, 3F; OSO_2CF_3). $^{13}\text{C}\{^1\text{H}\}$ NMR (CD_2Cl_2 , r.t., δ /ppm): 10.2 ($\text{C}_5(\text{CH}_3)_5$), 67.0 ($\text{C}_6\text{F}_4\text{HSO}_2\text{NCHPhCHPhNH}_2$), 75.7 ($\text{C}_6\text{F}_4\text{HSO}_2\text{NCHPhCHPhNH}_2$), 92.0 ($\text{C}_5(\text{CH}_3)_5$), 112.6, 120.3, 122.4 ($\text{C}_6\text{F}_4\text{H}$), 126.0, 126.4, 128.4, 128.7, 128.8 (Ph group), 135.9, 138.4 ($\text{C}_{\text{Ph}_{\text{ipso}}}$), 143.2, 144.0 ($\text{C}_6\text{F}_4\text{H}$). Anal. Calcd for $\text{C}_{31}\text{H}_{30}\text{F}_7\text{IrN}_2\text{O}_5\text{S}_2$: C, 41.38; H, 3.36; N, 3.11. Found: C, 41.29; H, 3.36; N, 3.09.

Synthesis of $\text{Cp}^*\text{Ir}[\kappa^2(\text{N}, \text{N}', \text{C})-(\text{S}, \text{S})-\text{C}_6\text{F}_3\text{HSO}_2\text{NCHPhCHPhNH}_2]$ (8**).** Formic acid (24.7 mg, 0.54 mmol) was added to a THF (30 mL) solution of **2b** (348.7 mg, 0.465 mmol) at room temperature, and the resulting solution was stirred at 70 °C for 20 h. The color of the solution changed from bright yellow to red-purple to finally orange. Then, the solution was cooled to room temperature, and triisopropylsilyl chloride (121.2 mg, 0.629 mmol) was added and stirred for 1 h at room temperature. The solvent was removed under reduced pressure and the resulting mixture was purified by silica gel column chromatography eluted with dichloromethane and methanol ($R_f = 0.35$ in TLC with $\text{CH}_2\text{Cl}_2/\text{MeOH} = 98/2$) to give $\text{Cp}^*\text{IrCl}[\kappa^2(\text{N}, \text{N}')-(\text{S}, \text{S})-\text{C}_6\text{F}_3\text{HSO}_2\text{NCHPhCHPhNH}_2]$ as a yellow powder in 2% yield (6.0 mg, 7.8×10^{-3} mmol). Subsequently, the product and silver fluoride (4.4 mg, 0.035 mmol) were dissolved in acetonitrile (5 mL), and the solution was stirred at 80 °C for a week. After drying up the solvent, the mixture was purified by column chromatography (silica gel, eluted with dichloromethane and methanol; $R_f = 0.75$ in TLC with DCM/MeOH = 98/2) and recrystallization from acetonitrile/diethyl ether to give the product **8** in 35% isolated yield (2 mg, 2.7×10^{-3} mmol) as yellow crystals. ^1H NMR (CD_2Cl_2 , r.t., δ /ppm): 1.79 (s, $\text{C}_5(\text{CH}_3)_5$, 15H), 3.17 (br t $^3J_{\text{HH}} = 12$ Hz, $\text{ArSO}_2\text{NCHPhCHPhNH}_2$, 1H), 3.56 (m, $\text{ArSO}_2\text{NCHPhCHPhNH}_2$, 1H), 4.09 (br d $^3J_{\text{HH}} = 10$ Hz, $\text{ArSO}_2\text{NCHPhCHPhNH}_2$, 1H), 6.78 (d $^3J_{\text{HH}} = 7.0$ Hz, aryl, 2H), 7.00–7.03 (m, aryl, 2H), 7.07–7.23 (m, aryl, 7H). ^{19}F NMR (CD_2Cl_2 , r.t., δ /ppm): –158.6 (apparent ddd, F^a , 1F), –140.2 (apparent d, F^b , 1F), –118.1 (apparent d, F^c , 1F). Anal. Calcd for $\text{C}_{30}\text{H}_{30}\text{F}_3\text{IrN}_2\text{O}_2\text{S}$: C, 49.24; H, 4.13; N, 3.83. Found: C, 48.90; H, 4.19; N, 3.70.

^{19}F NMR Monitoring Experiment of the Conversion from **3a to **4** (Figure 2).** In a NMR tube, formic acid (1.1 mg, 2.4×10^{-2} mmol) was added to a solution of FsDPEN -amido Ir complex **2a** (9.8 mg, 1.3×10^{-2} mmol) in THF- d_6 (0.45 mL). The color of the solution changed from red-purple (**2a**) to yellow (**3a**) to orange (**4**) via red-purple. The transformation was monitored by ^{19}F NMR as depicted in Figure 2.

Fluoride Trapping Experiment (Scheme 6). To a THF solution (10 mL) of $\text{FsDPEN-hydrido(amine)}$ complex **3a**, which was performed by treatment of amido complex **2a** (154.2 mg, 0.20 mmol) with formic acid (9.7 mg, 0.21 mmol) at $-30\text{ }^\circ\text{C}$ for 1 h; triisopropylsilyl chloride (38.9 mg, 0.20 mmol) was added and stirred for 9 h at room temperature. Then, the solvent was removed under reduced pressure, and the resulting yellow powder was washed with hexane ($3\text{ mL} \times 3$). The product (127.5 mg) was a mixture of chlorido complexes having FsDPEN and $\text{Fs}^{\text{H}}\text{DPEN}$ (69% yield, **1a**:**1b** = 5.9:1, determined by ^{19}F NMR as shown in Figure S5).

Cyclometalation Promoted by Fluoride (Schemes 10 and 11). *Method A.* In a NMR tube, $\text{Fs}^{\text{H}}\text{DPEN-chlorido(amine)}$ Ir complex **1b** (4.01 mg, 5.1×10^{-3} mmol) and silver fluoride (0.9 mg, 7.1×10^{-3} mmol) was mixed in CD_3CN (0.5 mL). The solution was soaked in an ultrasonic water bath for 30 min, and the solution was left to stand at room temperature.

Method B. To a premixed solution of cationic $\text{Fs}^{\text{H}}\text{DPEN-Ir}$ complex **7** (6.7 mg, 7.4×10^{-3} mmol) in CD_3CN (0.5 mL), tetra(*n*-butyl) ammonium fluoride (7.5 μL , 1 M solution in THF) was added. The solution was left to stand at room temperature. The ^{19}F NMR spectrum after 26 h is shown in Figure S6.

X-ray Crystallographic Measurements. All measurements were made on a Rigaku Saturn CCD area detector equipped with graphite-monochromated Mo $K\alpha$ radiation ($\lambda = 0.71075\text{ \AA}$) under nitrogen stream at 93 K. Indexing was performed from 18 images. The crystal-to-detector distance was 45.05 mm. The data were collected to a maximum 2θ value of 55.0° . A total of 720 oscillation images were collected. A sweep of data was carried out using ω scans from -110.0 to 70.0° in 0.5° steps, at $\chi = 45.0^\circ$ and $\phi = 0.0^\circ$. A second sweep was performed using ω scans from -110.0 to 70.0° in 0.5° steps, at $\chi = 45.0^\circ$ and $\phi = 90.0^\circ$. Intensity data were collected for Lorentz polarization effects as well as absorption. Structure solution and refinements were performed with the CrystalStructure program package. The heavy atom positions were determined by Direct methods (SIR2002), and the remaining non-hydrogen atoms were found by subsequent Fourier techniques. An empirical absorption correction based on equivalent reflections was applied to all data. All non-hydrogen atoms other than solvent molecules were refined anisotropically by full-matrix least-squares techniques based on F^2 using the CRYSTALS³¹ or SHELXL-2014³² program. All hydrogen atoms were constrained to ride on their parent atom. Relevant crystallographic data are compiled in Tables S1–S4.

■ ASSOCIATED CONTENT

Supporting Information

The Supporting Information is available free of charge on the ACS Publications website at DOI: 10.1021/acs.organomet.8b00242.

Experimental procedures and characterization data including NMR spectra of new compounds (PDF)

Accession Codes

CCDC 1834324–1834331 contain the supplementary crystallographic data for this paper. These data can be obtained free of charge via www.ccdc.cam.ac.uk/data_request/cif, or by emailing data_request@ccdc.cam.ac.uk, or by contacting The Cambridge Crystallographic Data Centre, 12 Union Road, Cambridge CB2 1EZ, UK; fax: +44 1223 336033.

■ AUTHOR INFORMATION

Corresponding Author

*E-mail: ykayaki@o.cc.titech.ac.jp

ORCID

Yoshihito Kayaki: 0000-0002-4685-8833

Shigeki Kuwata: 0000-0002-3165-9882

Author Contributions

All authors other than T.I. have given approval to the final version of the manuscript.

Notes

The authors declare no competing financial interest.

#T.I. deceased on April 21, 2017.

■ ACKNOWLEDGMENTS

This study was financially supported by the Japan Society for the Promotion of Science (JSPS) KAKENHI Grant Number 26621043 and 18K14225 and in part by a Grant for Engineering Research from Mizuho Foundation for the Promotion of Sciences and the Sasakawa Scientific Research Grant. A.M. is grateful to the JSPS for a Research Fellowship for Young Scientists (No. 17J09484). We thank the Material Analysis Suzukake-dai Center, Technical Department, Tokyo Institute of Technology, for HRMS analysis. We also acknowledge Takasago International Corporation for generous gifts of (*S,S*)-1,2-diphenylethylenediamine.

■ REFERENCES

- (1) (a) Hird, M. *Chem. Soc. Rev.* **2007**, *36*, 2070–2095. (b) Müller, K.; Faeh, C.; Diederich, F. *Science* **2007**, *317*, 1881–1886. (c) Purser, S.; Moore, P. R.; Swallow, S.; Gouverneur, V. *Chem. Soc. Rev.* **2008**, *37*, 320–330. (d) Prakash, G. K. S.; Wang, F.; O'Hagan, D.; Hu, J.; Ding, K.; Dai, L.-X. *Flourishing Frontiers in Organofluorine Chemistry*. In *Organic Chemistry: Breakthrough and Perspectives*, Ding, K., Dai, L.-X., Eds.; Wiley-VCH: Weinheim, Germany, 2012; pp 413–476. (e) Swallow, S. *Fluorine-Containing Pharmaceuticals*. In *Fluorine in Pharmaceutical and Medicinal Chemistry: From Biophysical Aspects to Clinical Applications*; Gouverneur, V., Müller, K., Eds.; Imperial College Press: London, 2012; pp 141–174. (f) Wang, J.; Sánchez-Roselló, M.; Aceña, J. L.; del Pozo, C.; Sorochinsky, A. E.; Fustero, S.; Soloshonok, V. A.; Liu, H. *Chem. Rev.* **2014**, *114*, 2432–2506. (g) Gillis, E. P.; Eastman, K. J.; Hill, M. D.; Donnelly, D. J.; Meanwell, N. A. *J. Med. Chem.* **2015**, *58*, 8315–8359.
- (2) (a) Liang, T.; Neumann, C. N.; Ritter, T. *Angew. Chem., Int. Ed.* **2013**, *52*, 8214–8264. (b) Campbell, M. G.; Ritter, T. *Chem. Rev.* **2015**, *115*, 612–633. (c) Yang, X.; Wu, T.; Phipps, R. J.; Toste, F. D. *Chem. Rev.* **2015**, *115*, 826–870. (d) Champagne, P. A.; Desroches, J.; Hamel, J.-D.; Vandamme, M.; Paquin, J.-F. *Chem. Rev.* **2015**, *115*, 9073–9174. (e) Yerien, D. E.; Bonesi, S.; Postigo, A. *Org. Biomol. Chem.* **2016**, *14*, 8398–8427. (f) Sather, A. C.; Buchwald, S. L. *Acc. Chem. Res.* **2016**, *49*, 2146–2157. (g) Kohlhepp, S. V.; Gulder, T. *Chem. Soc. Rev.* **2016**, *45*, 6270–6288.
- (3) (a) Shteingarts, V. D. *J. Fluorine Chem.* **2007**, *128*, 797–805. (b) Nova, A.; Mas-Ballesté, R.; Lledós, A. *Organometallics* **2012**, *31*, 1245–1256. (c) Kuehnel, M. F.; Lentz, D.; Braun, T. *Angew. Chem., Int. Ed.* **2013**, *52*, 3328–3348. (d) Whittlesey, M. K.; Peris, E. *ACS Catal.* **2014**, *4*, 3152–3159. (e) Weaver, J. D. *Synlett* **2014**, *25*, 1946–1952. (f) Hu, J.-Y.; Zhang, J.-L. *Top. Organomet. Chem.* **2015**, *52*, 143–196.
- (4) (a) Aizenberg, M.; Milstein, D. *Science* **1994**, *265*, 359–361. (b) Vela, J.; Smith, J. M.; Yu, Y.; Ketterer, N. A.; Flaschenriem, C. J.; Lachicotte, R. J.; Holland, P. L. *J. Am. Chem. Soc.* **2005**, *127*, 7857–7870. (c) Reade, S. P.; Mahon, M. F.; Whittlesey, M. K. *J. Am. Chem. Soc.* **2009**, *131*, 1847–1861. (d) Beltrán, T. F.; Feliz, M.; Llusar, R.; Mata, J. A.; Safont, V. S. *Organometallics* **2011**, *30*, 290–297. (e) Lv, H.; Zhan, J.-H.; Cai, Y.-B.; Yu, Y.; Wang, B.; Zhang, J.-L. *J. Am. Chem. Soc.* **2012**, *134*, 16216–16227. (f) Zhan, J.-H.; Lv, H.; Yu, Y.; Zhang, J.-L. *Adv. Synth. Catal.* **2012**, *354*, 1529–1541. (g) Zámostná, L.; Ahrens, M.; Braun, T. *J. Fluorine Chem.* **2013**, *155*, 132–142. (h) He, Y.; Chen, Z.; He, C.-Y.; Zhang, X. *Chin. J. Chem.* **2013**, *31*, 873–877. (i) Lv, H.; Cai, Y.-B.; Zhang, J.-L. *Angew. Chem., Int. Ed.* **2013**, *52*, 3203–3207. (j) Chen, Z.; He, C.-Y.; Yin, Z.; Chen, L.; He, Y.; Zhang, X. *Angew. Chem., Int. Ed.* **2013**, *52*, 5813–5817. (k) Podolan, G.; Lentz, D.; Reissig, H.-U. *Angew. Chem., Int. Ed.* **2013**, *52*, 9491–9494.

- (l) Arévalo, A.; Tlahuext-Aca, A.; Flores-Alamo, M.; García, J. J. *J. Am. Chem. Soc.* **2014**, *136*, 4634–4639. (m) Schwartzburd, L.; Mahon, M. F.; Poulten, R. C.; Warren, M. R.; Whittlesey, M. K. *Organometallics* **2014**, *33*, 6165–6170. (n) Podolan, G.; Jungk, P.; Lentz, D.; Zimmer, R.; Reissig, H.-U. *Adv. Synth. Catal.* **2015**, *357*, 3215–3228. (o) Alfonso, C.; Beltrán, T. F.; Feliz, M.; Llusar, R. *J. Cluster Sci.* **2015**, *26*, 199–209. (p) McKay, D.; Riddlestone, I. M.; Macgregor, S. A.; Mahon, M. F.; Whittlesey, M. K. *ACS Catal.* **2015**, *5*, 776–787. (q) Cybulski, M. K.; Riddlestone, I. M.; Mahon, M. F.; Woodman, T. J.; Whittlesey, M. K. *Dalton Trans.* **2015**, *44*, 19597–19605. (r) Cybulski, M. K.; Nicholls, J. E.; Lowe, J. P.; Mahon, M. F.; Whittlesey, M. K. *Organometallics* **2017**, *36*, 2308–2316. (s) Cybulski, M. K.; McKay, D.; Macgregor, S. A.; Mahon, M. F.; Whittlesey, M. K. *Angew. Chem., Int. Ed.* **2017**, *56*, 1515–1519. (t) Hein, N. M.; Pick, F. S.; Fryzuk, M. D. *Inorg. Chem.* **2017**, *56*, 14513–14523.
- (5) (a) Breyer, D.; Braun, T.; Penner, A. *Dalton Trans.* **2010**, *39*, 7513–7520. (b) Wu, J.; Cao, S. *ChemCatChem* **2011**, *3*, 1582–1586. (6) (a) Yow, S.; Gates, S. J.; White, A. J. P.; Crimmin, M. R. *Angew. Chem., Int. Ed.* **2012**, *51*, 12559–12563. (b) Ekkert, O.; Strudley, S. D. A.; Rozenfeld, A.; White, A. J. P.; Crimmin, M. R. *Organometallics* **2014**, *33*, 7027–7030.
- (7) Catalytic HDF of perfluoroaromatic substrates: (a) Mai, V. H.; Nikonov, G. I. *ACS Catal.* **2016**, *6*, 7956–7961. (b) Chen, J.; Huang, D.; Ding, Y. *ChemistrySelect* **2017**, *2*, 1219–1224. (c) Liu, X.; Wang, Z.; Zhao, X.; Fu, X. *Inorg. Chem. Front.* **2016**, *3*, 861–865.
- (8) Catalytic HDF of partially fluorinated substrates: (a) Ukisu, Y.; Miyadera, T. *J. Mol. Catal. A: Chem.* **1997**, *125*, 135–142. (b) Kuhl, S.; Schneider, R.; Fort, Y. *Adv. Synth. Catal.* **2003**, *345*, 341–344. (c) Sawama, Y.; Yabe, Y.; Shigetura, M.; Yamada, T.; Nagata, S.; Fujiwara, Y.; Maegawa, T.; Monguchi, Y.; Sajiki, H. *Adv. Synth. Catal.* **2012**, *354*, 777–782. (d) Sabater, S.; Mata, J. A.; Peris, E. *Nat. Commun.* **2013**, *4*, 2553–2559. (e) Sabater, S.; Mata, J. A.; Peris, E. *Organometallics* **2015**, *34*, 1186–1190.
- (9) Li, J.; Zheng, T.; Sun, H.; Li, X. *Dalton Trans.* **2013**, *42*, 13048–13053.
- (10) Matsunami, A.; Kuwata, S.; Kayaki, Y. *ACS Catal.* **2016**, *6*, 5181–5185.
- (11) (a) Ahrens, T.; Kohlmann, J.; Ahrens, M.; Braun, T. *Chem. Rev.* **2015**, *115*, 931–972. (b) Amii, H.; Uneyama, K. *Chem. Rev.* **2009**, *109*, 2119–2183. (c) Kiplinger, J. L.; Richmond, T. G.; Osterberg, C. E. *Chem. Rev.* **1994**, *94*, 373–431. (d) Chen, W.; Bakewell, C.; Crimmin, M. R. *Synthesis* **2017**, *49*, 810–821. (e) Shen, Q.; Huang, Y.-G.; Liu, C.; Xiao, J.-C.; Chen, Q.-Y.; Guo, Y. *J. Fluorine Chem.* **2015**, *179*, 14–22. (f) Stahl, T.; Klare, H. F. T.; Oestreich, M. *ACS Catal.* **2013**, *3*, 1578–1587. (g) Unzner, T. A.; Magauer, T. *Tetrahedron Lett.* **2015**, *56*, 877–883. (h) Weaver, J.; Senaweera, S. *Tetrahedron* **2014**, *70*, 7413–7428. (i) Braun, T.; Wehmeier, F. *Eur. J. Inorg. Chem.* **2011**, *2011*, 613–625.
- (12) (a) Cronin, L.; Higgitt, C. L.; Karch, R.; Perutz, R. N. *Organometallics* **1997**, *16*, 4920–4928. (b) Park, S.; Roundhill, M. *Inorg. Chem.* **1989**, *28*, 2905–2906. (c) Barrios-Francisco, R.; Benítez-Páez, T.; Flores-Alamo, M.; Arévalo, A.; García, J. J. *Chem. - Asian J.* **2011**, *6*, 842–849. (d) Zhang, W.-H.; Zhang, X.-H.; Tan, A. L.; Yong, M. A.; Young, D. J.; Hor, T. S. A. *Organometallics* **2012**, *31*, 553–559. (e) Johnson, S. A.; Taylor, E. T.; Cruise, S. J. *Organometallics* **2009**, *28*, 3842–3855. (f) Johnson, S. A.; Huff, C. W.; Mustafa, F.; Saliba, M. J. *Am. Chem. Soc.* **2008**, *130*, 17278–17280. (g) Fischer, P.; Götz, K.; Eichhorn, A.; Radius, U. *Organometallics* **2012**, *31*, 1374–1383. (h) Schaub, T.; Backes, M.; Radius, U. *Eur. J. Inorg. Chem.* **2008**, *2008*, 2680–2690. (i) Schaub, T.; Backes, M.; Radius, U. *J. Am. Chem. Soc.* **2006**, *128*, 15964–15965. (j) Braun, T.; Izundu, J.; Steffen, A.; Neumann, B.; Stammer, H.-G. *Dalton Trans.* **2006**, 5118–5123. (k) Breyer, D.; Braun, T.; Kläring, P. *Organometallics* **2012**, *31*, 1417–1424.
- (13) (a) Deacon, G. B.; Forsyth, C. M.; Sun, J. *Tetrahedron Lett.* **1994**, *35*, 1095–1098. (b) Kiplinger, J. L.; Richmond, T. G. *Chem. Commun.* **1996**, 1115–1116. (c) Senaweera, S. M.; Singh, A.; Weaver, J. D. *J. Am. Chem. Soc.* **2014**, *136*, 3002–3005. (d) Arora, A.; Weaver, J. D. *Acc. Chem. Res.* **2016**, *49*, 2273–2283.
- (14) Edelbach, B. L.; Rahman, A. K. F.; Lachicotte, R. J.; Jones, W. D. *Organometallics* **1999**, *18*, 3170–3177.
- (15) σ -Bond metathesis of C–F bonds with Z-type ligands: (a) Kameo, H.; Ikeda, K.; Bourissou, D.; Sakaki, S.; Takemoto, S.; Nakazawa, H.; Matsuzaka, H. *Organometallics* **2016**, *35*, 713–719. (b) Kameo, H.; Kawamoto, T.; Sakaki, S.; Bourissou, D.; Nakazawa, H. *Chem. - Eur. J.* **2016**, *22*, 2370–2375. (c) Kameo, H.; Baba, Y.; Sakaki, S.; Bourissou, D.; Nakazawa, H.; Matsuzaka, H. *Organometallics* **2017**, *36*, 2096–2106.
- (16) Krüger, J.; Leppkes, J.; Ehm, C.; Lentz, D. *Chem. - Asian J.* **2016**, *11*, 3062–3071.
- (17) (a) Kraft, B. M.; Lachicotte, R. J.; Jones, W. D. *J. Am. Chem. Soc.* **2001**, *123*, 10973–10979. (b) Kraft, B. M.; Jones, W. D. *J. Organomet. Chem.* **2002**, *658*, 132–140.
- (18) (a) Whittlesey, M. K.; Perutz, R. N.; Moore, M. H. *Chem. Commun.* **1996**, 787–788. (b) Edelbach, B. L.; Jones, W. D. *J. Am. Chem. Soc.* **1997**, *119*, 7734–7742. (c) Rieth, R. D.; Brennessel, W. W.; Jones, W. D. *Eur. J. Inorg. Chem.* **2007**, *2007*, 2839–2847. (d) Maron, L.; Werkema, E. L.; Perrin, L.; Eisenstein, O.; Andersen, R. A. *J. Am. Chem. Soc.* **2005**, *127*, 279–292. (e) Werkema, E. L.; Andersen, R. A. *J. Am. Chem. Soc.* **2008**, *130*, 7153–7165. (f) Diggle, R. A.; Kennedy, A. A.; Macgregor, S. A.; Whittlesey, M. K. *Organometallics* **2008**, *27*, 938–944. (g) Li, B. Z.; Qian, Y. Y.; Liu, J. W.; Chan, K. S. *Organometallics* **2014**, *33*, 7059–7068. (h) Jäger-Fiedler, U.; Klahn, M.; Arndt, P.; Baumann, W.; Spannenberg, A.; Burlakov, V. V.; Rosenthal, U. *J. Mol. Catal. A: Chem.* **2007**, *261*, 184–189. (i) Procacci, B.; Jiao, Y.; Evans, M. E.; Jones, W. D.; Perutz, R. N.; Whitwood, A. C. *J. Am. Chem. Soc.* **2015**, *137*, 1258–1272. (j) Barrio, P.; Castarlenas, R.; Esteruelas, M. A.; Lledos, A.; Maseras, F.; Oñate, E.; Tomás, J. *Organometallics* **2001**, *20*, 442–452. (k) Peterson, T. H.; Golden, J. T.; Bergman, R. G. *Organometallics* **1999**, *18*, 2005–2020.
- (19) (a) Fahey, D. R.; Mahan, J. E. *J. Am. Chem. Soc.* **1977**, *99*, 2501–2508. (b) Burling, S.; Elliott, P. I. P.; Jasim, N. A.; Lindup, R. J.; McKenna, J.; Perutz, R. N.; Archibald, S. J.; Whitwood, A. C. *Dalton Trans.* **2005**, 3686–3695. (c) Steffen, A.; Sladek, M. I.; Braun, T.; Neumann, B.; Stammer, H.-G. *Organometallics* **2005**, *24*, 4057–4064. (d) Archibald, S. J.; Braun, T.; Gaunt, J. A.; Hobson, J. E.; Perutz, R. N. *J. Chem. Soc., Dalton Trans.* **2000**, 2013–2018. (e) Sladek, M. I.; Braun, T.; Neumann, B.; Stammer, H.-G. *J. Chem. Soc., Dalton Trans.* **2002**, 297–299. (f) Hatnean, J. A.; Johnson, S. A. *Organometallics* **2012**, *31*, 1361–1373. (g) Johnson, S. A.; Mroz, N. M.; Valdivia, R.; Murray, S. *Organometallics* **2011**, *30*, 441–457. (h) Jasim, N. A.; Perutz, R. N.; Whitwood, A. C.; Braun, T.; Izundu, J.; Neumann, B.; Rothfeld, S.; Stammer, H.-G. *Organometallics* **2004**, *23*, 6140–6149. (i) Schaub, T.; Radius, U. *Chem. - Eur. J.* **2005**, *11*, 5024–5030. (j) Nova, A.; Reinhold, M.; Perutz, R. N.; Macgregor, S. A.; McGrady, J. E. *Organometallics* **2010**, *29*, 1824–1831. (k) Yoshikai, N.; Mashima, H.; Nakamura, E. *J. Am. Chem. Soc.* **2005**, *127*, 17978–17979. (l) Nakamura, Y.; Yoshikai, N.; Iliés, L.; Nakamura, E. *Org. Lett.* **2012**, *14*, 3316–3319. (m) Braun, T.; Perutz, R. N.; Sladek, M. I. *Chem. Commun.* **2001**, 2254–2255. (n) Noveski, D.; Braun, T.; Neumann, B.; Stammer, H.-G. *Dalton Trans.* **2004**, 4106–4119. (o) Raza, A. L.; Panetier, J. A.; Teltewskoi, M.; Macgregor, S. A.; Braun, T. *Organometallics* **2013**, *32*, 3795–3807.
- (20) (a) Koike, T.; Ikariya, T. *Adv. Synth. Catal.* **2004**, *346*, 37–41. (b) Matsunami, A.; Kayaki, Y.; Ikariya, T. *Chem. - Eur. J.* **2015**, *21*, 13513–13517.
- (21) (a) Haack, K.-J.; Hashiguchi, S.; Fujii, A.; Ikariya, T.; Noyori, R. *Angew. Chem., Int. Ed. Engl.* **1997**, *36*, 285–288. (b) Matsunami, A.; Kuwata, S.; Kayaki, Y. *ACS Catal.* **2017**, *7*, 4479–4484.
- (22) (a) Christie, K. O.; Wilson, W. W. *J. Fluorine Chem.* **1990**, *46*, 339–342. (b) Shenderovich, I. G.; Smirnov, S. N.; Denisov, G. S.; Gindin, V. A.; Golubev, N. S.; Dunger, A.; Reibke, R.; Kirpekar, S.; Malkina, O. L.; Limbach, H.-H. *Ber. Bunsenges. Phys. Chem.* **1998**, *102*, 422–428.
- (23) Arisawa, M.; Ichikawa, T.; Yamaguchi, M. *Tetrahedron Lett.* **2013**, *54*, 4327–4329.
- (24) Examples of fluoridoiridium(III) complexes: (a) Doherty, N. M.; Hoffmann, N. W. *Chem. Rev.* **1991**, *91*, 553–573. (b) Veltheer, J.

- E.; Burger, P.; Bergman, R. G. *J. Am. Chem. Soc.* **1995**, *117*, 12478–12488. (c) Caulton, K. G. *New J. Chem.* **1994**, *18*, 25–41. (d) Fawcett, J.; Harding, D. A. J.; Hope, E. G.; Singh, K.; Solan, G. A. *Dalton Trans.* **2010**, *39*, 10781–10789. (e) Baumgarth, H.; Meier, G.; Braun, T.; Braun-Cula, B. *Eur. J. Inorg. Chem.* **2016**, *2016*, 4565–4572. (f) Maity, A.; Stanek, R. J.; Anderson, B. L.; Zeller, M.; Hunter, A. D.; Moore, C. E.; Rheingold, A. L.; Gray, T. G. *Organometallics* **2015**, *34*, 109–120. (g) Patel, B. P.; Crabtree, R. H. *J. Am. Chem. Soc.* **1996**, *118*, 13105–13106.
- (25) Koike, T.; Ikariya, T. *Organometallics* **2005**, *24*, 724–730.
- (26) (a) Cooper, A. C.; Folting, K.; Huffman, J. C.; Caulton, K. G. *Organometallics* **1997**, *16*, 505–507. (b) Grushin, V. V.; Marshall, W. J. *J. Am. Chem. Soc.* **2004**, *126*, 3068–3069.
- (27) (a) Eisenstein, O.; Milani, J.; Perutz, R. N. *Chem. Rev.* **2017**, *117*, 8710–8753. (b) Pike, S. D.; Crimmin, M. R.; Chaplin, A. B. *Chem. Commun.* **2017**, *53*, 3615–3633.
- (28) (a) Clot, E.; Eisenstein, O.; Jasim, N.; Macgregor, S. A.; McGrady, J. E.; Perutz, R. N. *Acc. Chem. Res.* **2011**, *44*, 333–348. (b) Reinhold, M.; McGrady, J. E.; Perutz, R. N. *J. Am. Chem. Soc.* **2004**, *126*, 5268–5276.
- (29) Dub, P. A.; Wang, H.; Matsunami, A.; Gridnev, I. D.; Kuwata, S.; Ikariya, T. *Bull. Chem. Soc. Jpn.* **2013**, *86*, 557–568.
- (30) Martins, J. E. D.; Wills, M. *Tetrahedron* **2009**, *65*, 5782–5786.
- (31) Carruthers, J. R.; Rollett, J. S.; Betteridge, P. W.; Kinna, D.; Pearce, L.; Larsen, A.; Gabe, E. *CRYSTALS Issue 11*; Chemical Crystallography Laboratory: Oxford, U.K., 1999.
- (32) Sheldrick, G. M. *Acta Crystallogr., Sect. C: Struct. Chem.* **2015**, *71*, 3–8.